

# CHALMERS



## **Powder Material for Inductor Cores**

**Evaluation of MPP, Sendust and High flux core characteristics**

*Master of Science Thesis*

JOHAN KINDMARK  
FREDRIK ROSÉN

Department of Energy and Environment  
*Division of Electric Power Engineering*  
CHALMERS UNIVERSITY OF TECHNOLOGY  
Göteborg, Sweden 2013



# **Powder Material for Inductor Cores**

## **Evaluation of MPP, Sendust and High flux core characteristics**

JOHAN KINDMARK  
FREDRIK ROSÉN

Department of Energy and Environment  
Division of Electric Power Engineering  
CHALMERS UNIVERSITY OF TECHNOLOGY  
Göteborg, Sweden 2013

Powder Material for Inductor Cores  
Evaluation of MPP, Sendust and High flux core characteristics  
JOHAN KINDMARK  
FREDRIK ROSÉN

© JOHAN KINDMARK  
FREDRIK ROSÉN, 2013.

Department of Energy and Environment  
Division of Electric Power Engineering  
Chalmers University of Technology  
SE-412 96 Göteborg  
Sweden  
Telephone +46 (0)31-772 1000

Chalmers Bibliotek, Reproservice  
Göteborg, Sweden 2013

Powder Material for Inductor Cores  
Evaluation of MPP, Sendust and High flux core characteristics  
JOHAN KINDMARK  
FREDRIK ROSÉN  
Department of Energy and Environment  
Division of Electric Power Engineering  
Chalmers University of Technology

## **Abstract**

The aim of this thesis was to investigate the performance of alternative powder materials and compare these with conventional iron and ferrite cores when used as inductors. Permeability measurements were performed where both DC-bias and frequency were swept, the inductors were put into a small buck converter where the overall efficiency was measured. The BH-curve characteristics and core loss of the materials were also investigated. The materials showed good performance compared to the iron and ferrite cores. High flux had the best DC-bias characteristics while Sendust had the best performance when it came to higher frequencies and MPP had the lowest core losses. Sendust had the overall best results when comparing all materials and another positive aspect is that they are not limited in which shapes they can be made.

**Index term:** Core materials, High flux, Inductor, MPP, Powder cores, Sendust



## **Acknowledgements**

First of all we would like to thank our tutor Anders Thorsén for all the help and feedback he has provided during the whole progress of this thesis. We would like to thank our examiner Torbjörn Thiringer for his guidance and feedback regarding the report. We would also like to thank Benny Stegefelt for his help with contact information for the supplier, Lennart Kruse for his input regarding inductors and Johan Håkansson for his everyday advices. Lastly we would like to thank the Power Solution at Ericsson Lindholmen for supplying us the resources needed to complete our work. The work has been carried out at Ericsson Lindholmen.

Johan Kindmark & Fredrik Rosén  
Göteborg, Sweden, 2013





## **Abbreviations**

AC - Alternating current

CCM - Continuous conduction mode

DC - Direct current

DCM - Discontinuous conduction mode

EMI - Electro magnetic interference

MOSFET - Metal oxide semiconductor field effect transistor

MPP - Molypermalloy powder

PCB - Printed circuit board

PWM - Pulse width modulation



# Contents

<b>Abstract</b>	<b>iii</b>
<b>Acknowledgements</b>	<b>v</b>
<b>Abbreviations</b>	<b>vii</b>
<b>Contents</b>	<b>ix</b>
<b>1 Introduction</b>	<b>1</b>
1.1 Background . . . . .	1
1.2 Aim . . . . .	1
1.3 Scope . . . . .	1
1.4 Method . . . . .	1
<b>2 Technical Background</b>	<b>3</b>
2.1 The inductor and important magnetic concepts . . . . .	3
2.1.1 The magnetisation curve . . . . .	4
2.1.2 Hysteresis losses . . . . .	6
2.1.3 Eddy currents and the resistive losses . . . . .	6
2.2 Different Inductor Types . . . . .	7
2.3 Core Materials . . . . .	7
2.3.1 Ferrite Cores . . . . .	8
2.3.2 Powder Cores . . . . .	8
2.4 Thermal aging and temperature dependence . . . . .	9
2.5 Design Considerations . . . . .	10
2.6 Buck Converter . . . . .	11

Contents

<b>3</b>	<b>Test Subjects</b>	<b>13</b>
<b>4</b>	<b>Frequency Measurements</b>	<b>15</b>
4.1	Test Setup . . . . .	15
4.2	Measurements . . . . .	15
4.2.1	Inductance deviation for individual materials . . . . .	15
4.2.2	Inductance deviation comparing different materials . . . . .	18
4.3	Analysis and discussion . . . . .	19
<b>5</b>	<b>DC-Bias Measurements</b>	<b>21</b>
5.1	Test Setup . . . . .	21
5.2	Measurements . . . . .	21
5.2.1	Permeability deviations . . . . .	22
5.2.2	Inductance Changes . . . . .	24
5.3	Analysis and discussion . . . . .	27
<b>6</b>	<b>Buck Converter Measurements</b>	<b>29</b>
6.1	Test Setup . . . . .	29
6.2	Measurements . . . . .	29
6.2.1	Permeability Comparison . . . . .	29
6.2.2	Material Comparison . . . . .	31
6.2.3	High Current Buck Converter . . . . .	33
6.2.4	Frequency Sweep in Buck Converter . . . . .	34
6.3	Analysis and discussion . . . . .	35
<b>7</b>	<b>BH-curve Measurements</b>	<b>37</b>
7.1	Test Setup . . . . .	37
7.2	Results . . . . .	38
7.2.1	BH-curve . . . . .	38
7.2.2	Core losses . . . . .	39
7.3	Analysis and Discussion . . . . .	40

<b>8</b>	<b>Categorisation</b>	<b>43</b>
<b>9</b>	<b>Conclusion</b>	<b>45</b>
9.1	Future Work . . . . .	45
	<b>References</b>	<b>47</b>

## Contents

# **1. Introduction**

## **1.1 Background**

In the telecom field there is a demand to increase the efficiency and make the Printed Circuit Boards, PCB, more compact. As of today a large part of the board is occupied by the power stage, which supplies the board with its different voltage levels. There is a need to make more efficient and compact power stages and the inductor does not show the same energy storage vs size as the rest of the design. One trend is that the voltages in the circuit is lowered and therefore a higher current is needed to keep the same power level. These two considerations puts higher requirements on the inductor and it is therefore interesting to investigate alternative core materials.

Traditionally ferrites with air gap have been used as choke inductors in the power stages. The major concern with ferrites is that they saturate early. This can be solved by increasing the air gap but this will increase the overall losses of the component. Powder materials, such as iron powder, Sendust, Molypermalloy Powder, MPP, and High flux saturates at higher levels. The powder materials have distributed air gaps which are built up by small particles which have been bound together. This organic binder has been the major problem since it has deteriorated over time and reduced the performance of the inductor. Lately the technology has improved by replacing the organic binder with a non-organic binder [1]. By using alternative powder materials the aim is to reduce the size of the inductor but maintain the performance.

## **1.2 Aim**

The aim of this thesis is to investigate, test and analyse the performance of inductor coils constructed of alternative powder alloys. These will then be compared with conventional ferrite and iron powder cores.

## **1.3 Scope**

In this thesis the materials investigated will be used in choke inductors and the materials will be limited to ferrites, iron powder, Sendust, MPP and High flux cores. Nanocrystalline materials will be mentioned but will not be put to the test due to their working conditions being lower frequency applications. Due to the fact that some of the powder materials are limited to toroidal shaped cores all core materials acquired will have this shape. The tests performed has been limited to investigate the electrical and magnetically properties of these materials and thus temperature dependance will not be investigated physically but it will be discussed.

## **1.4 Method**

To achieve the goal of this thesis a thorough literature study has to be concluded to give good knowledge of the inductor, the various materials suitable for evaluation as well as for the different test setups needed to conclude the measurements.

## *Chapter 1. Introduction*

When the materials have been acquired, the toroidal cores will be wound with copper wire to actual inductors. The inductors will be wound to a couple of different sizes. They will then be run through two tests where the frequency and the DC-bias current are changed respectively in order to get the inductance variation of the materials. After that, the BH-curves will be measured to see when the material saturates as well as the losses in the core of the inductor. The inductors will also be mounted in an actual converter to see the performance in a real application.

When all measurements are performed, the results will be analysed and compared with theoretical data of the powder materials as well as with performance from inductors using more conventional materials. When the comparisons of the different materials are completed, they will then be categorised for suitable applications of operations.



## 2. Technical Background

This chapter will describe the relevant theory needed for this thesis. The first part will describe the inductor and how ferromagnetic materials behave under different magnetisation levels. The next part will describe different kinds of inductors as well as the materials used in the cores that are investigated and how they are affected when stressed with high temperatures. The later part handles general design considerations for inductors as well as the different converter topologies the inductors are supposed to be operating in.

### 2.1 The inductor and important magnetic concepts

The derivation of the inductor is taken from the book *Solid State Tesla Coil* by Gary L. Johnson [2]. An inductor is an electrical component which stores energy in a magnetic field. An inductor usually consists of a conductor that is wound around a magnetic core. From circuit theory the voltage,  $V_L$ , created by the current,  $i$ , across the inductor can be expressed as

$$V_L = L \frac{di}{dt} \quad (2.1)$$

where  $L$  is the inductance of the inductor. Another way to explain the same voltage is to use Faraday's law which says that

$$V_L = N \frac{d\Phi}{dt} \quad (2.2)$$

where  $N$  is the number of turns of the conductor and  $\Phi$  is the magnetic flux flowing through the coil. By putting these equations together one gets

$$Li = N\Phi \quad (2.3)$$

where the left side is the circuit quantities and the right is the field quantities. The inductance can then be expressed as

$$L = N \frac{\Phi}{i} \quad (2.4)$$

The relation between  $\Phi$  and  $i$  is nonlinear when using ferromagnetic materials and it is important to connect this equation with the magnetic flux density,  $B$ , and the field intensity,  $H$ . The magnetic flux can be expressed as

$$\Phi = \iint B dA \quad (2.5)$$

If the magnetic flux density is even across the core the equation simply becomes

$$\Phi = BA \quad (2.6)$$

where  $A$  is the cross sectional area of the core. The magnetic flux density can then be expressed as

$$B = \mu_0 \mu_r H \quad (2.7)$$

where  $\mu_0$  is the permeability of vacuum and  $\mu_r$  is the relative permeability of the core material. The relative permeability is the prime factor when determining the amount of energy that the inductor can store, especially when the space for the inductor is limited. The energy stored can be expressed as

$$W = \frac{1}{2}LI^2 \quad (2.8)$$

Finally, the connection of the magnetising force and the current flowing in the inductor can be expressed according to Ampere's law as

$$Ni = \oint Hdl \quad (2.9)$$

This equation states that the current equals the integral of the magnetising force surrounded by an arbitrary part  $dl$ . If the loop  $dl$  surrounds the full inductor current the equation becomes

$$Ni = Hl \quad (2.10)$$

where  $l$  is the mean magnetic path length in the core of the inductor. The relation between the flux density and the magnetising force is best described using the magnetisation curve, especially for ferromagnetic materials because of the nonlinearity of the material.

### 2.1.1 The magnetisation curve

The following explanation of magnetisation curves and magnetic domains is an important concept when understanding how magnetic material behaves and most of the theory are gathered from *Field and Wave Electromagnetics* by David Cheng [3].

A typical magnetisation curve, or BH-curve, can be studied in figure 2.1. It can be seen that the BH-curve is only linear for a small part of the applied magnetising force. This is because the magnetic material saturate which means that the relative permeability approaches that of air and less energy can be stored in the core. This implies that the permeability will decrease when the linearity between the flux density and the magnetising force deviates. The inductance decreases with the permeability since the magnetic flux stays constant (2.6). When the material is fully saturated the inductor can be regarded as short circuit. It is therefore important when designing inductors to have a safe distance between the operating point and the saturation point. Various materials have different BH characteristics which make them suitable for different applications. All magnetic materials have hysteresis and resistive losses but the magnitude of these depends on the materials and the electrical conditions. Magnetic materials have a saturation point where the flux density no longer increases. For ferrites this value is about 0.3 T and for iron 1.8 T [4].

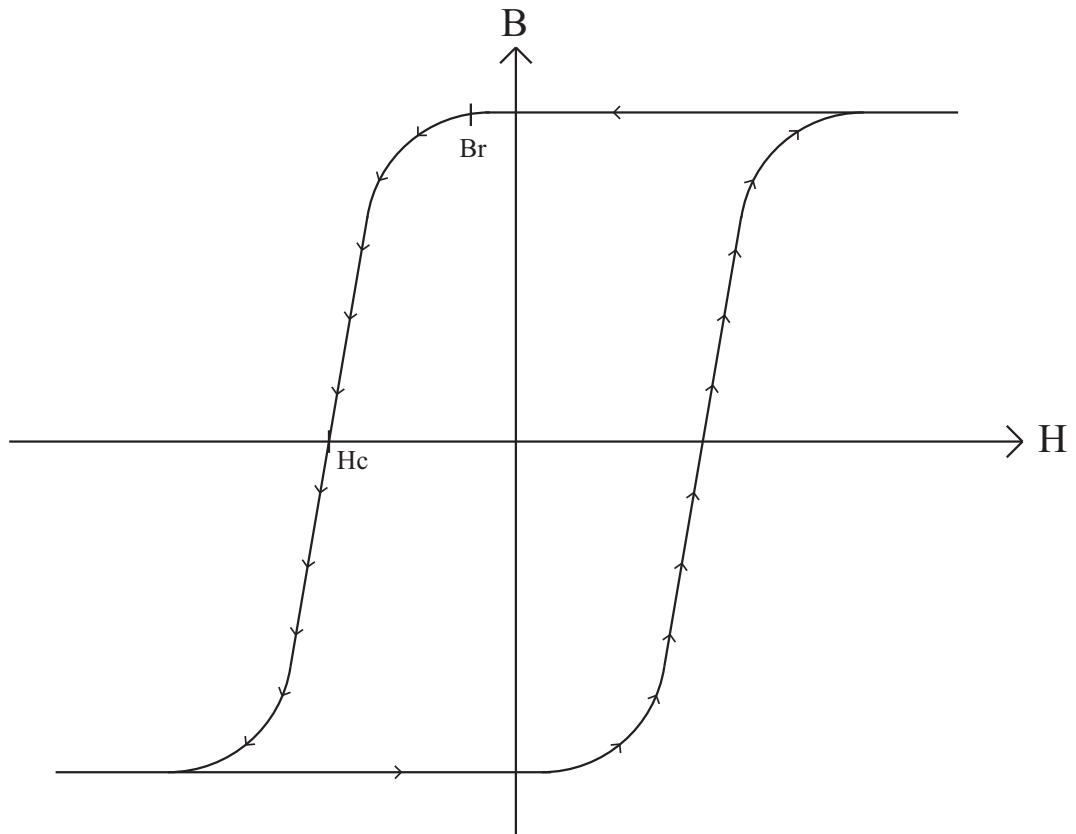


Fig. 2.1 A typical shape for a BH-curve.  $B_r$  represents the remnant flux density and  $H_c$  is the reversed field required to get the flux density back to zero.

The reason for the saturation in ferromagnetic materials can be explained by using the model of magnetic domains, see figure 2.2. Each of the domains consists of  $10^{15}$  to  $10^{16}$  atoms and they are fully magnetised in a sense since all magnetic dipoles made from spinning electrons in one domain is aligned in the same direction, even without any applied magnetic field. Between the different domains there are domain walls, which are about 100 atoms thick. When the material is demagnetised the different domains have the magnetic moments in different directions which can be seen in figure 2.2a. The net sum of the random magnetic moments will result in no magnetisation of the material.

When an external magnetic field is applied to the ferromagnetic material the walls of the domains, which are aligned with the external field, will grow at the expense of other domains. This will increase the magnetic flux. When the fields are weak the domain movement is reversible, but when reaching a certain point the movements will be non-reversible. When this happens the domains will start to rotate in the same direction as the applied field seen in figure 2.2b. When the applied field becomes zero the flux density will not go back to zero but instead reach a level  $B_r$  which is called the remanent flux density. To get the flux density back to zero an external field  $H_c$  has to be applied but in the opposite direction, the required strength is called coercive force. If all domains are aligned with the external field the material has reached saturation and the flux density cannot be higher, no matter how big the applied field as shown in figure 2.1.

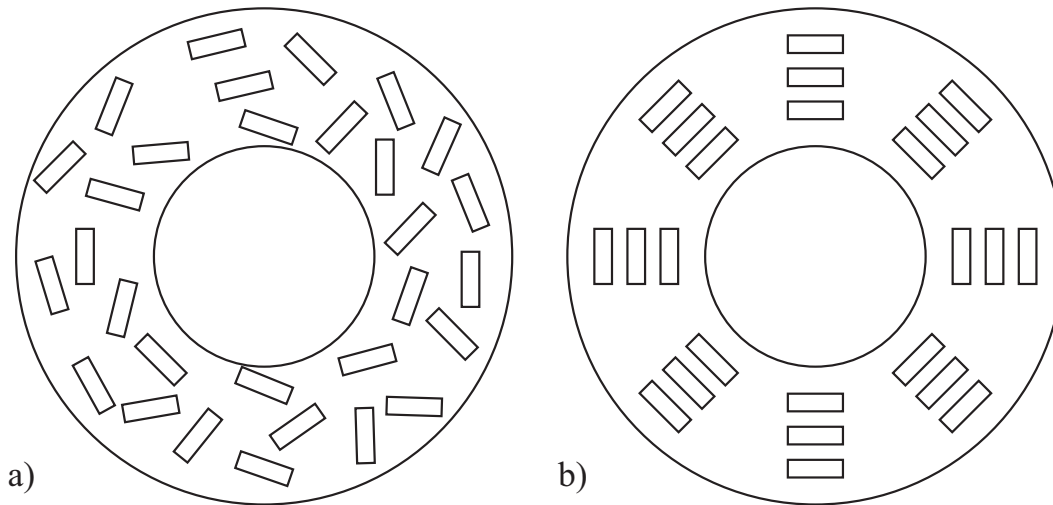


Fig. 2.2 Figure a) shows the magnetic domains with no external electric field applied and b) shows the magnetic domains when the material has reach saturation.

### 2.1.2 Hysteresis losses

Hysteresis losses are heat losses which occurs when the domains are aligning with the applied field. The heat is created from the friction of the movement. In switching applications, such as, transformers and electric motors it is important to have narrow hysteresis loops i.e large flux density from small applied fields since the applied field will range from  $\pm\Delta H_{ac}$  in each switching cycle and with high frequency the losses will be high. For the same material a higher permeability tends to lead to higher core losses [4]. The width of the magnetisation curve also affects the losses in the core. Materials that have narrow loops are called soft materials and material with wide loops are called hard. The hard materials are used for permanent magnets, while soft is used for transformers and inductors.

When the ferromagnetic material is exposed to a DC-biased field with an AC component, the operating point in BH-curve will be located depending on the field strength  $H_{dc}$  which is dependent on the DC-current. The applied field will change according to the rippling AC-current and the applied field will change between  $H_{dc} \pm\Delta H_{ac}$ . This will cause a minor hysteresis loop around the operating point. The flux density will then change between  $B_{dc} \pm\Delta B_{ac}$ . This can cause the material to reach saturation if the operation point is close to the limit of the material. An inductor with the same material, but different permeability, will get a different slope but the same saturation limit, hence if an air gap is introduced the maximum flux density will not change [4].

### 2.1.3 Eddy currents and the resistive losses

Eddy currents will affect both the core and the resistive losses of the windings. Eddy currents which are induced currents in the core inherits from the flux around the conductor. These currents produces heat in the core and can be reduced by using core material that has a high resistance which reduces the current induced in the core [5].

Eddy currents will also be created in the wires of the conductor. These can be seen as the resistive AC losses. The total resistive losses originate from both the DC and the AC resistance where the DC losses  $P_{dc}$ , can be expressed as

$$P_{dc} = R_{dc}I_{rms}^2 \quad (2.11)$$

where  $R_{dc}$  is the DC resistance and  $I_{rms}$  is the rms value of the DC-current. The AC resistance is more complex and it depends on both the skin effect of the wire as well as the proximity effect and both these effects increases with higher frequencies. The skin effect causes the actual area that the current uses in the conductor to shrink because the current is pushed away from the middle of the inductor. This is due to that the current creates an alternating magnetic field around the conductor. When the current changes, this magnetic field will create an electric field directed opposite to the current intensity. This electric field is strongest in the center of the conductor and thus the current is pushed to the edges. When choosing the size of the conductor it is important to know the skin depth which is the length the current will penetrate into the conductor and it can be calculated as

$$d = \sqrt{\frac{\rho}{\pi\omega\mu_0}} \quad (2.12)$$

where  $\rho$  is the resistivity of the material and  $\omega$  is the angular frequency of the current. If the skin depth is smaller than the radius of the conductor the skin effect will affect the current distribution [6].

The proximity effect occurs when conductors are put close to each other, for instance in an inductor with many turns of the conductor. The magnetic field created by the current will induce eddy currents in nearby conductors and this will change the current distribution overall. Current will be focused in areas in the conductors furthest away from nearby conductors which will decrease the area the current uses [7]. This increases the resistance which is defined as

$$R = \frac{\rho l}{A_e} \quad (2.13)$$

where  $\rho$  is the resistivity of the material,  $l$  is the length of the conductor and  $A_e$  is the cross sectional area of the conductor. Since both  $\rho$  and  $l$  are constant, the total resistance of the conductor increases when the area diminishes.

## 2.2 Different Inductor Types

The inductor core can have different geometries, for instance E, U, C, I, toroidal and block shapes. All shapes have different advantages and disadvantages and it is mainly depending on the application on what shape to chose [8]. Toroidal cores, as an example, has a closed magnetic path which will limit the induced field to escape but they require special machinery for the winding to be effective. When constructing an inductor, the traditional way is to wound the conducting wires around the magnetic core. Nowadays there is a type of inductor called composite inductors and these are created backwards seen from the traditional way of constructing [9]. When creating a composite inductor the conductors are wounded around an air coil and the edges are connected to a lead frame which serves as the mounting pads as well as the connection to the board. The core material, which are made by powders, are then pressed around the coil to give the inductor its square shape. Note that powder materials is not only used for composite inductors.

## 2.3 Core Materials

There exists a lot of various magnetic core materials and some common ones are ferrites, iron laminations, silicon steel and different powder materials, which is the main focus in this thesis. There is a high variance of the characteristics between the materials and what to chose depends on the application, saturation and the limit in physical size as mentioned in section 2.1. Some big manufacturer of these are Magnetics, Micrometals and Ferroxcube [4].

Another aspect to consider is at what temperatures the core will be exposed for. For magnetic material there is a very distinguished temperature known as the Curie temperature,  $T_c$ , named after the French scientist

Pierre Curie [3]. When a ferromagnetic material reaches  $T_c$  it loses its magnetisation and the material will have the same characteristics as a paramagnetic material with  $\mu_r$  around 1. Materials used in inductor cores usually has a  $T_c$  between 130 – 1000°C.

### 2.3.1 Ferrite Cores

The name ferrite is a collection of magnetic materials that consists of iron oxide, for example the hematite  $\text{Fe}_2\text{O}_3$ , where iron oxide is mixed with another material such as magnesium, zinc, nickel and barium [10]. The frequency range that ferrites are used in is wide, from kHz to GHz [11]. Ferrites have high resistivity which reduces the eddy current losses since it is harder for the current to be induced in the core itself. Nickel-zinc ferrites have the highest resistivity and is used for the highest frequencies. Magnesium-zinc is used for frequencies up to 5 MHz. A drawback of ferrites is its low saturation limit at around 0.3 T and they have a very clear breakpoint for the permeability. When they reach saturation the inductance value will plummet rapidly [12].

Ferrite materials are located on the lower end for Curie temperatures and it has its highest permeability just before  $T_c$ . Even though the magnetisation is lost above the Curie temperature no permanent damage will be dealt to the ferrite material. The change is only in the magnetic properties and not in the physical structure of the material. However, the physical structure may crack if the material is exposed for rapid change of its temperatures, at above 4° C per minute [13].

### 2.3.2 Powder Cores

Powder material can consists of different chemical elements in order to obtain the properties required of the core. With powder material, the air gap in the core will be distributed evenly across the whole core instead of a gapped part which is the case in a standard ferrite core [12]. The distributed air gap will give the material a better temperature stability as well as lower flux leakage. They also have a smoother reduction of its permeability but it starts much earlier compared to ferrites. They are also good from an EMI point of view since a discrete air gap can interfere with other part of the system. The permeability of the core depends on the size of the powder particles and the smaller the particle the lower the permeability becomes. Powder cores usually has its margin of error of the inductance specified to  $\pm 8\%$  [14].

#### Iron Powder

Iron powder used in magnetic cores consists of pure iron, Fe, and it is built up of small particles which is isolated from each other [15]. There exist different types of iron powder, for instance hydrogen reduced and carbonyl iron [16]. The carbonyl iron is usually used in RF, radio frequency, applications since they have good temperature stability where as the hydrogen reduced iron commonly is used for DC-chokes, mainly because of their higher permeability. Iron powder has rather high losses compared to the other powder materials but this can be compensated for applications where size is not an issue and when low cost is important. Iron powder saturates between 1-1.5 T and usually has a relative permeability ranging between 1-90 $\mu$ . One major drawback with iron powder has been that the binder used for isolating the grain particles, typically epoxy, is organic and thereby is exposed for thermal aging [12]. This makes the material sensitive for high temperatures, usually above 125° C, and this will cause the material to change its magnetic properties. Recent studies on new binding material has pushed the temperatures and some manufactures now guarantee that their cores is aging free up to 200° C [17], more about thermal aging can be seen in section 2.4.

#### MPP ( Molypermalloy Powder)

Molypermalloy powder, MPP, was introduced in 1940 and was first used to compensate the capacitance from long telephone lines [18]. The core is very stable when it comes to flux density, DC-current and

temperature. MPP generally has the lowest losses of all the powder materials and is used when a higher saturation level is needed without increasing the losses. The drawback is the cost, which is many times more than that of conventional ferrites, and the geometry which is limited to toroidal shapes. According to Magnetics [14], their MPP cores consists of a mix of 2% molybdenum, 17% iron and 81% nickel and the relative permeability ranges from 14-550. The frequency spectrum varies depending on which manufacturers specification that is regarded. Magnetics says that the range for their cores goes up to 1 MHz whereas Micrometals only goes up to 200 kHz [19].

### **High flux**

High flux cores consists of 50% iron and 50% nickel powder and is used when very high saturation, 1.5 T, is needed [20]. The losses is higher compared to MPP but much lower than the iron powder. High flux cores are the best powder cores when it comes to keep its permeability when the DC-bias is increased. Because of the permeability of the material, High flux cores are smaller than the standard iron powder core which makes it more suitable in applications where space is an issue. High flux cores have relative permeabilities between 14-160 $\mu$  and a frequency range up to 200 kHz [14] [19]. High flux cores is, like the MPP core, only available in toroidal shapes.

### **Sendust**

Sendust cores, also called Kool Mu cores, was invented in Japan 1936 and consists of 85% iron, 9% silicon and 6% aluminum [18]. They saturate at around 1T and they fit between iron powder and High flux cores when it comes to both losses and cost. The available relative permeabilities for Sendust cores are between 26-125 $\mu$ . Sendust is cheaper than both MPP and High flux because their is no nickel in the alloy which makes the production process easier. Sendust are available in toroidal and E shape cores as well as block shapes [19]. The frequency range is again different between Magnetics and Micrometals which states the range to 500 kHz and 1 MHz respectively [19] [21].

### **Nanocrystalline**

Nanocrystalline cores were first showed in 1988 when a group of Japanese scientists added small amounts of copper, Cu, and niob, Nb, to a standard Fe-Si-B amorphous alloy [22]. The reason for calling the material nanocrystalline is that the grain size of the powder is very small, from 10-100 nm. Nanocrystalline materials available in the market today are Nanoperm, Vitroperm, Hitperm and Finemet. The nanocrystalline materials shines in the lower frequency ranges, making them ideal for transformers and common mode chokes for inverter drives as well as high power applications [23]. Nanocrystalline materials will not be investigated further in this report but it is an interesting material that might develop further and thus it may be useful for higher frequency applications.

## **2.4 Thermal aging and temperature dependance**

The aging of core material depends on the binding material of the powder [24]. In iron powder the binding material is constructed of epoxy which often is organic and is therefore affected by the heat in core that can lead to thermal aging . When the binder has been exposed to high temperature, the core losses will increase [25]. Once the core has been affected by high temperature the process is irreversible i.e the core losses will increase with time. Therefore it is important to stay within the temperature limit when operating with iron powder. Iron powder as an example has an curie temperature of over 700°C but the binder that holds the particles together, which usually is epoxy or phenol, has a considerable lower temperature limit. This limit has been around 125° C but manufacturers now claims to have binders that can withstand temperatures up to 200°C [26] [24].

The Curie temperature for powder materials, such as MPP, Sendust and High flux is between 450-500° C [21] but the most important part is that the binder that keep the grains together is non organic which makes it non affected by thermal aging [19] [14]. The rated temperature is still usually put to 200° C because of the epoxy finish at the surface of the core [13]. The fact that these material does not inherit the thermal aging effect until 200°C make them ideal for working operations with continuously high temperatures.

Another important aspect to consider when it comes to temperatures is the change in permeability that might occur. This will change the performance of the inductor which in turn will affect the output ripple. If comparing the powder materials MPP has the best temperature stability with a change of only 2% at 200° C where High flux and Sendust deviates 4% and 8% respectively [13], this comparison is for the 125μ. An interesting observation is that the permeability increases for both MPP and High flux where as it declines for Sendust. The deviation in temperature is also greater for higher permeabilities.

## 2.5 Design Considerations

This section will discuss different aspects of inductor design and inspiration is taken from *Switching Power Supply Design* by Abraham I. Pressman [4]. For inductor design there are several aspects to consider. Which application should it be used for and what ratings such as current, voltage, frequency shall the inductor operate under. Other considerations are core size, cost and losses which is aspects the engineer usually has to make a trade off between.

To determine the initial inductance, i.e. no bias current or frequency, of an inductor designers often use something called the AL value. The relation is described as

$$L = A_L N^2 \quad (2.14)$$

where  $L$  is the inductance,  $N$  is the number of turns of the conductor and  $AL$  is the AL value for the specific core material. The AL value depends on the permeability of the materials as well as the geometric dimensions and is given by the manufacturer of the cores.

As mentioned in section 2.1.1 the DC bias point will affect the permeability of the core material. Another parameter that will change the inductance value is the operation frequency. Manufacturers usually present the inductance variations for both frequency and current but the frequency is kept low when the DC bias is swept and vice versa. Hence the calculated inductance value may differ from the actual. Therefore one should test the inductor in the actual circuit to make sure its characteristics is within the limits of the design.

When designing an inductor for a buck converter, a major factor for the performance of the inductor is the output DC-current. The inductance is usually kept high in order to get a smooth output current without ripple. In cases with a high output current, where the inductance decline one can either increase the turn ratio or use a higher permeability material. With a higher permeability one problem is that permeability will have a larger deviation when the current changes due to the fact that the initial permeability declines earlier. The other case will increase the losses of the inductor since a higher amount of turns means longer conductor and thus higher resistive losses.

When it comes to the frequency of the application there are some general guidelines that may be followed. When the frequency is low, usually iron powder is used because of high saturation flux density, low hysteresis and eddy losses as well as the cheap cost of the material. At really high frequencies ferrites are used because of their lower core losses. For higher frequency the diameter of the wire is another important aspect since the skin effect will occur.

When designing inductors there are generally two approaches used, core loss limited and copper loss limited. Which one of the two that is used depends on where the majority of the losses in the design will be



located. When the current ripple or the frequency is low there will not be any major losses in the core, instead the design is limited by the copper losses in the windings. This is the copper loss limited approach and is often used with buck converters because of the high DC current and there will be significant resistive losses in the windings according to (2.11). It is, in this case, important to use a wire with a large cross sectional area to reduce the resistance (2.13). There is a trade off since if a thick wire is used, less turns can be fit into the core which will lower the inductance or alternatively a larger core as to be used. The core loss limited approach is used when the frequency is high and the core material will have a high impact on the losses. In these cases materials with smaller area of the its BH loop is suitable.

This is only a small fraction of the issues the designer is confronted with and there is a lot of different things to think about which makes the design processes of the inductor both difficult and important for the overall performance of the circuit.

## 2.6 Buck Converter

The inductors investigated in this thesis is usually used as output chokes in DC-DC converters. The applications studied is mostly converters where the voltage is transformed to a lower level and the inductors have been tested in different buck converters. The theory presented is mostly gathered from *Power Electronics: Converters, Applications and Design* by N. Mohan et.al [7]. The theory only describes the behavior of the circuit and not the logic needed to switch the transistor in the converter. The buck converter is one of the simplest converters that can be used. It consists of a switch, often a Metal oxide semiconductor field effect transistor, MOSFET, a diode, a capacitor and an output inductor. The schematics can be seen in 2.3.

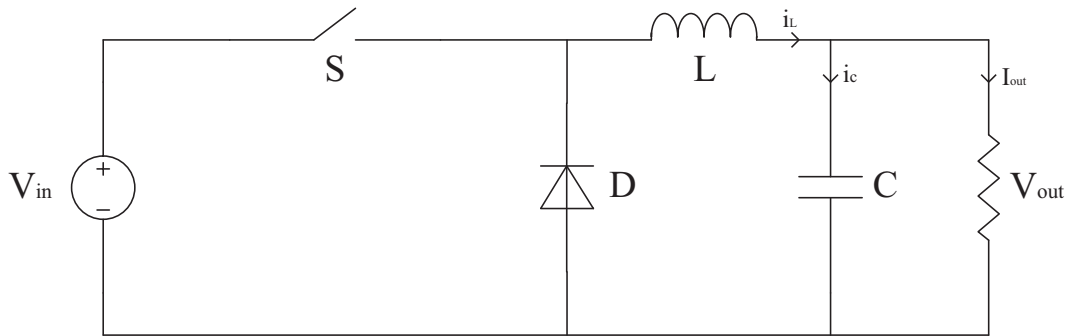


Fig. 2.3 The ideal circuit diagram of a Buck converter.

The principle is that the switch is conducting for a certain amount of time, depending on the input voltage and the desired voltage on the output. In steady state the voltage across the inductor has to be zero for a whole period. For continuous conduction mode, CCM, i.e when the current through the inductor flows during the whole period, the relation between the voltages can be derived as

$$\begin{aligned}
 0 &= \frac{1}{T} \int V_L dt = \frac{1}{T} \left( \int_0^{DT} (V_d - V_0) dt + \int_{DT}^T -V_0 dt \right) = \\
 &= \frac{1}{T} ((V_d - V_0)DT - V_0T - (-V_0)DT) \leftrightarrow \frac{V_0}{V_d} = D
 \end{aligned} \tag{2.15}$$

where  $V_L$  is the voltage across the inductor,  $V_0$  is the output voltage,  $D$  is the duty cycle,  $V_d$  is the input

## *Chapter 2. Technical Background*

voltage and  $T$  is the period of the switching frequency. The voltage is usually monitored and controlled by a drive circuit with pulse width modulation, PWM.

There is also a possibility to run the converter in discontinuous conduction mode, DCM, where the energy stored in the inductor is discharged before the ending of the period, resulting that  $i_L$ , the current through the inductor, is zero for a short while before the next period. This may be suitable in applications with high switching losses since the losses when the MOSFET is turned on is negligible.

### 3. Test Subjects

In this chapter the data description of the different cores used for the inductors will be presented. The same cores will be used for rest of the tests in this thesis unless otherwise specified. When selecting the inductors the goal was to get them as similar as possible regarding both size and permeability. In Table 3.1 the different materials used are described with their specific values. For the rest of this thesis when permeabilities are mentioned it will simply be written as  $26\mu$ ,  $60\mu$ ,  $125\mu$  etc. and it then tells the relative permeability of the mentioned core. For the tests it was decided that the inductance values should be 2 and  $10\mu$  because of the available buck converters. The wire used is a standard copper wire with a diameter of 1.2 mm, except for the BH measurements where the number of turns were much higher and a 0.7 mm diameter wire was used. The number of turns is calculated from equation (2.14).

Table 3.1: Characteristics of the cores used in the tests

Material	Iron	Ferrite	MPP	High flux	Sendust
$\mu_r$	35, 75	125	26, 60, 125	26, 60, 125	60, 125
Outer Diameter [mm]	20.2	23.7	21.1	21.1	21.1
Inner Diameter [mm]	12.6	13.1	12.0	12.0	12.0
Cross Section Area [mm <sup>2</sup> ]	24.3	39.75	22.1	22.1	22.1
Mean Path Length [mm]	51.5	57.8	50.9	50.9	50.9
Cost [£]	1.01, 0.32	-	1.97	1.26	0.66
AL [nH/turn]	18, 45	87	14, 32, 68	14, 32, 68	14, 32, 68
Turns $2\mu$	11, 7	6	12, 8, 6	12, 8, 6	12, 8, 6
Turns $10\mu$	24, 15	12	27, 18, 12	27, 18, 12	27, 18, 12

The iron cores are manufactured by Amidon where the  $35\mu$  is an iron mix called carbonyl HP often denoted as -3 and  $75\mu$  is a hydrogen reduced iron powder denoted as -26. These were the only two cores available with the correct size and reasonable permeability compared to the other powder materials.

The ferrite core used is called 4C65, TN23/14/7 from Ferroxcube. It is an ungapped core and it was chosen since it resembles the other powder cores in both size and permeability. Ferrite cores are often gapped to get a lower permeability when used as output inductors but to make the comparison as equal as possible the toroidal shape was chosen.

The MPP, Sendust and High flux cores are from both Arnold Magnetics and Magnetics Inc. The reason there is no  $26\mu$  Sendust is that it was not available at the time the materials were acquired. Note that for the MPP, Sendust and High flux cores only one prize is given since the cost is defined by the size of the core. The reason for not presenting a cost for the ferrite core is that a price was only found in a Swedish store and is therefore unfair to compare it with a English distributer where the other core were acquired.

*Chapter 3. Test Subjects*

## 4. Frequency Measurements

This chapter will describe the frequency measurements and how the frequency affects the permeability of the material. This is interesting since the switching frequencies in converters and the operating frequencies for different applications can vary from kHz to MHz and these may effect the core materials.

### 4.1 Test Setup

The frequency will be swept from 10 kHz - 2 MHz using an LCR meter, Agilent 4980A. The instrument has a four terminal pair configuration which reduces the influence of stray inductance which occur at higher frequencies. The four terminals are low current, low potential, high current and high potential respectively. The terminals for the low side is connected together to one side of the test object and the high side to the other. Before any inductor is tested both short and open calibrations are performed on the LCR meter. For the short calibration a shortening board, provided by the manufacturer, is connected to the four terminals. The frequency sweep will be divided into 201 values, which is the maximum for this instrument. While the frequency is swept both the current and the voltage will be very low, in the micro or milli regions.

### 4.2 Measurements

The frequency measurement result has been divided into two categories. The first compares each material separately for different permeabilities and the inductance change as a function of applied frequency. In the second part the different materials are compared to each other. The change of the inductance will be presented as a percentage of the initial inductance value.

#### 4.2.1 Inductance deviation for individual materials

When looking at figure 4.1 it is seen that the 35 $\mu$  iron is stable across the complete test range. The 75 $\mu$  iron declines rapidly when reaching 200 kHz.

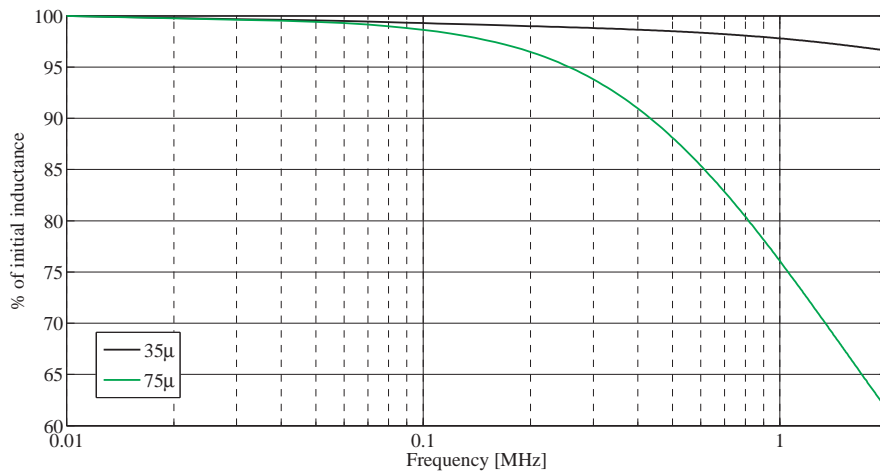


Fig. 4.1 The change in inductance for 35µ and 75µ iron cores when the frequency is swept from 10 kHz to 2 MHz.

From figure 4.2 it is apparent that the ferrite is stable over a big range of frequencies, this is no surprise since ferrite cores are often used for high frequency applications. One interesting phenomenon is the spikes in the inductance at 90 kHz and 700 kHz. This is believed to be the self resonance of the inductor, which may depend on the stray capacitance of the core and of the windings. The phenomenon is described in [27] and the measured inductance shape is similar to the one in the article. The reason for the different peak values of the spikes may be because of the different winding resistance in the two inductors.

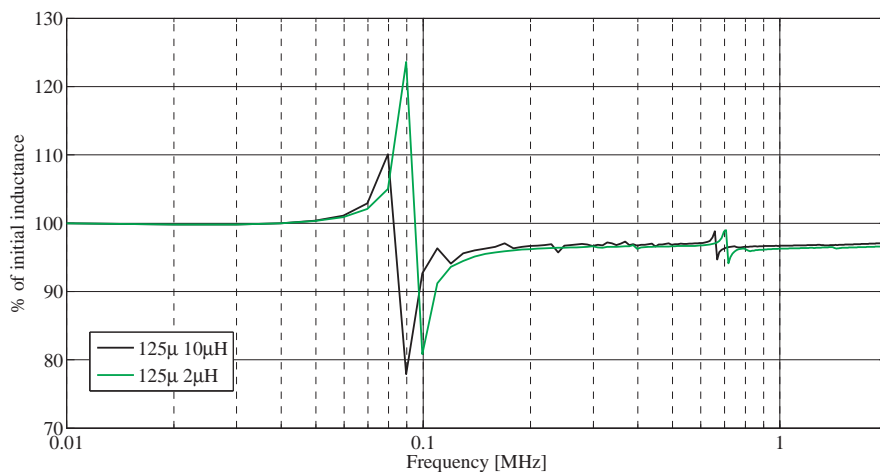


Fig. 4.2 The change in inductance for the 125µ ferrite core with 2 and 10 µH when the frequency is swept from 10 kHz to 2 MHz.

In figure 4.3 it can be seen that the 60µ and the 125µ cores are equal up to 150 kHz and after that the 125µ core starts to decline. One can also see that the 26µ core has the lowest inductance until 250 kHz and is lower than 60µ to around 1 MHz where it passes.

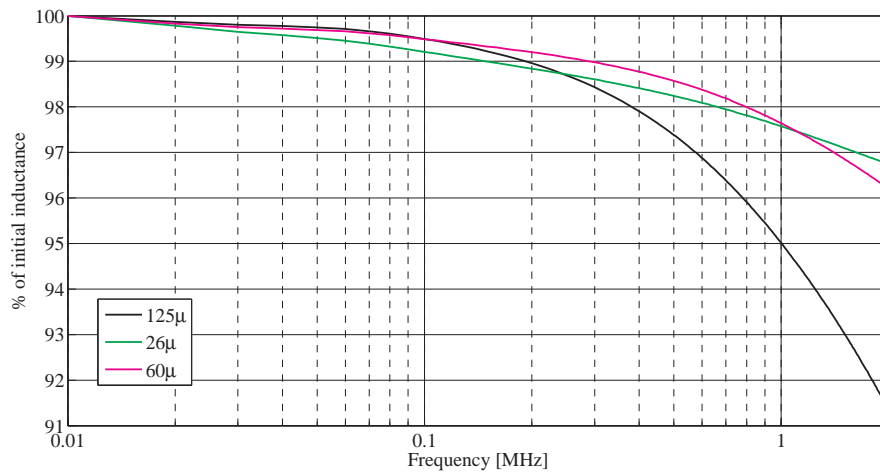


Fig. 4.3 The change in inductance for 26µ, 60µ and 125µ MPP cores when the frequency is swept from 10 kHz to 2 MHz.

The High flux cores, seen in figure 4.4 follows the same pattern as the MPP cores with 26µ being lower in the beginning and then take over as the most consistent after 200 kHz. The 26µ and 60µ cores drops to 96.5% and 93% respectively which can be seen as a rather good result since the frequency range is, according Magnetics Inc. [21], between 60 Hz - 200 kHz.

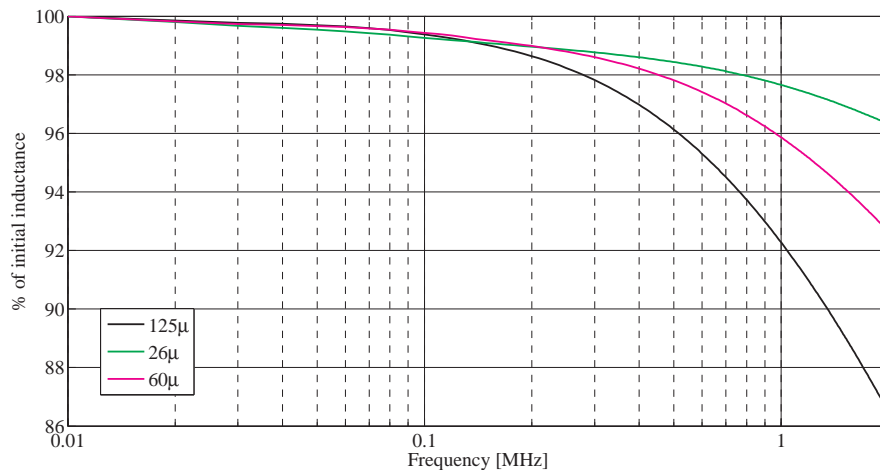


Fig. 4.4 The change in inductance for 26µ, 60µ and 125µ High flux cores when the frequency is swept from 10 kHz to 2 MHz.

The Sendust cores can be seen in figure 4.5 and they perform well compared to the other powder materials. The 60µ core only declines 1.5% at 2 MHz whereas the 125µ reduces by 6%. The most interesting thing to note is that the 60µ have not reached the frequency where the more rapid reduction starts to take place which is the case for the 125µ core does.

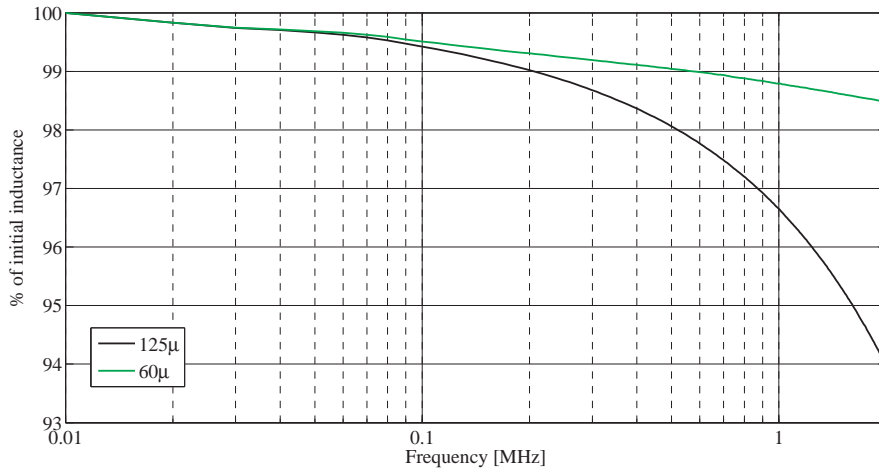


Fig. 4.5 The change in inductance for 60µ and 125µ Sendust cores when the frequency is swept from 10 kHz to 2 MHz.

### 4.2.2 Inductance deviation comparing different materials

In figure 4.6 it is evident that all the material keeps a high inductance through the whole test range and they are packed tightly together, within 1% difference at 2 MHz. For the lower frequencies MPP has a lower value then the other two materials but it overtakes at around 1.6 MHz.

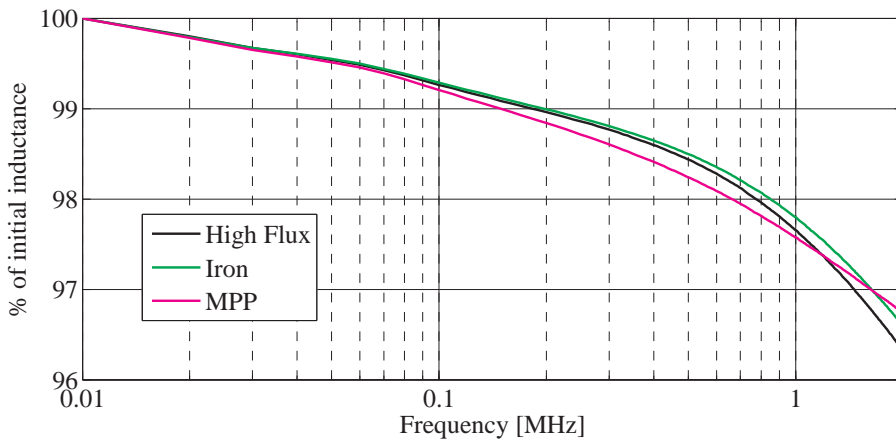


Fig. 4.6 The change in inductance for the 26µ MPP and High flux and 35µ iron when the frequency is swept from 10 kHz to 2 MHz.

When comparing 60µ cores and both of the iron cores, one can see that Sendust clearly has the best performance for higher frequency when it comes to keep up the initial permeability with a value of 98.5% at 2 MHz. The iron and MPP core is located directly after with a reduction to 96.2% and 96.6% respectively, followed by the High flux at 92.6%. The iron 75µ is by far the worst material when it comes to higher frequencies since it starts to decline even below 100 kHz.



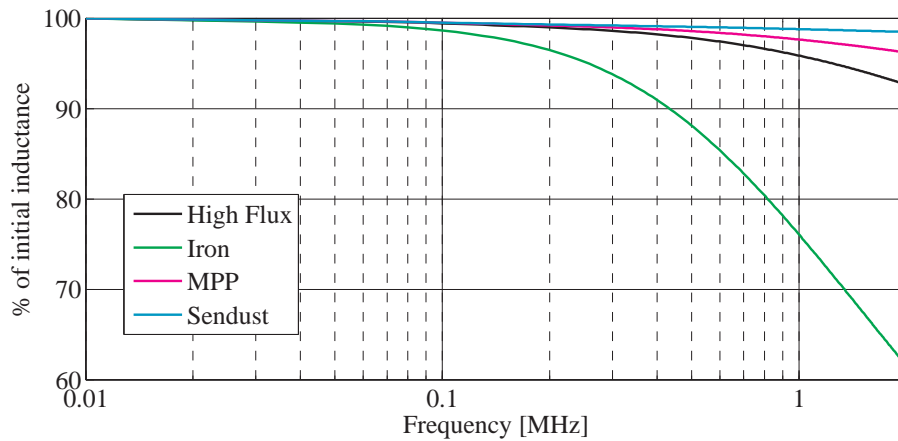


Fig. 4.7 The change in inductance for the 60 $\mu$  MPP, Sendust and High flux and 75 $\mu$  iron when the frequency is swept from 10 kHz to 2 MHz.

In figure 4.8 it is apparent that the 75 $\mu$  iron core has the largest decline in inductance. It is extra interesting since it is compared to the 125 $\mu$  of the other cores since higher permeability materials in general declines faster than the lower permeabilities, see figure 4.1 - 4.5. The ferrite core keeps its inductance curve flat during the whole frequency range, but it has diminished a few % after the resonance spikes. For the alloy powders Sendust is the one with the best performance with a 94% of its initial inductance remaining at 2 MHz, closely followed by MPP at 91.4% and High flux a little bit lower at 86.5%.

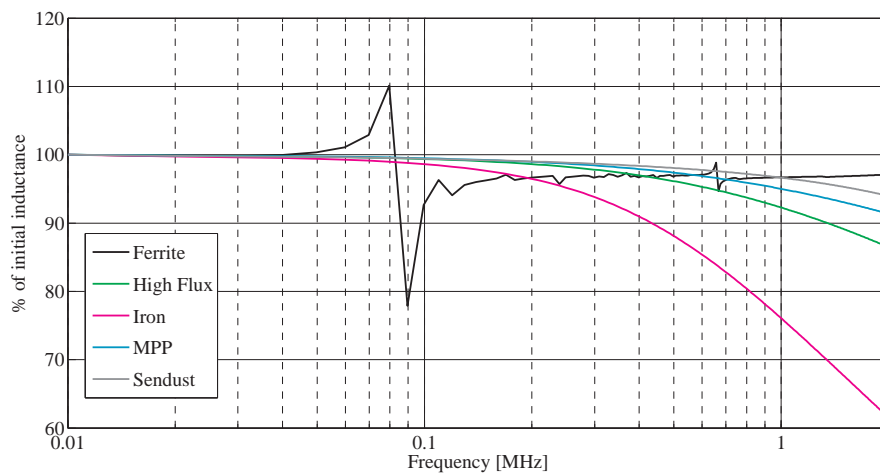


Fig. 4.8 The change in inductance for the 75 $\mu$  iron and the 125 $\mu$  MPP, Sendust, High flux and ferrite when the frequency is swept from 10 kHz to 2 MHz.

### 4.3 Analysis and discussion

When it comes to the frequency it is clear that the ferrite and Sendust cores have the best performance but as seen in figure 4.8 the spikes in the ferrite plot has to be considered. Since this ferrite core is the only one tested there is no telling if this behavior is spread through out other ferrite cores or if it is a specific characteristic for the particular core. The overall performance of the powder materials is good and the differences between them is quite small.

#### Chapter 4. Frequency Measurements

When it comes to the frequency specification for the different powder materials the manufacturer sets a rather low number on the frequency range, see section 2.3.2. From the tests it is clear that the permeability deviation is not the main factor for the manufacturer when they set their frequency limit but it may be the core losses that has the largest impact. Generally the frequency is kept down because of the core losses during the switching and not the permeability deviation of the core itself but nowadays the switching frequencies for converters are pushed to the MHz range which will effect the cores and this has to be accounted for when constructing the circuit.

A comparison between the measured values and the manufacturer [28] [29] values can be seen in table 4.1. It shows the permeability deviation at 1 MHz and the difference between the measured and the provided values are quite small. The largest deviation is that Micrometals values for MPP and High flux is considerably lower for the 125 $\mu$ . The values from both manufacturer are estimated from graphs and may not be fully accurate.

Table 4.1: Comparison between measured and manufacture values at 1 MHz. The result is presented as % of the initial permeability.

	Measured Value [%]	Data Sheet Magnetics [%]	Data Sheet Micrometals [%]
MPP 26 $\mu$	97.7	98	99
MPP 60 $\mu$	97.6	98	96
MPP 125 $\mu$	95	93	86
High flux 26 $\mu$	97.5	98	98
High flux 60 $\mu$	95.8	96	90
High flux 125 $\mu$	92.4	93	84
Sendust 60 $\mu$	98.8	99	98
Sendust 125 $\mu$	96.6	97	96

## 5. DC-Bias Measurements

In this chapter the DC-currents effect on the permeability will be investigated. The reason for doing these tests is to see how the material behave under various current conditions since the inductors operate under different conditions and these test may indicate where the materials has their optimal operating condition.

### 5.1 Test Setup

The DC-bias current is varied from 0-20 A with a step length of 0.2 A and the inductance is measured with an inductance analyser 3245 from Wayne Kerr. The inductance analyser is fed with two parallel DC-supplies at 20 A each.

The magnetising force is calculated in Oersted which is defined as

$$H = \frac{4\pi I}{1000l_m} \quad (5.1)$$

where  $I$  is the current and  $l_m$  is the mean magnetic path length of the core. The reason for plotting the permeability deviation against the magnetising force is that both the number of turns and the current are accounted for and thus makes the comparison more general and Oerstedt is used because most of the manufacturer use it in their data sheets. The relative permeability,  $\mu_r$  is calculated from the measured inductance values as

$$\mu_r = \frac{l_m L}{\mu_0 A_e N^2} \quad (5.2)$$

where  $L$  is the measured inductance,  $\mu_0$  is the permeability of free space,  $A_e$  is the cross sectional area of the core and  $N$  is the number of turns of the conductor. The number of turns for the different permeabilities can be seen in table 3.1

### 5.2 Measurements

The DC-bias test have been divided into two categories. In the first the permeability deviation of the materials are shown. The different materials are shown separately. In the second part the deviation of the inductance is presented. The materials are compared against one another and the plots are instead divided with respect to the relative permeability.

The inductance change is directly proportional to the change in permeability, since the permeability change is derived from the inductance measurements. The reason for showing these plots is to give background for the test with the buck converter because it is easier to see what happens with the inductor at different currents. The idea at this stage was to use a buck converter that had an output inductor at 10  $\mu\text{H}$  but this got changed afterwards. The measurements was already performed and thus the were chose to be presented and compared with the 2  $\mu\text{H}$  which is the value of the output inductor on the converter used.

### 5.2.1 Permeability deviations

In figure 5.1 the permeability deviation is shown for the two iron cores and one interesting observation that can be made is that both iron cores increases their permeability for lower magnetising forces. It is not by much, just around 2 % for the 35 $\mu$  core. It is also clear that the higher permeability drops faster than the lower one.

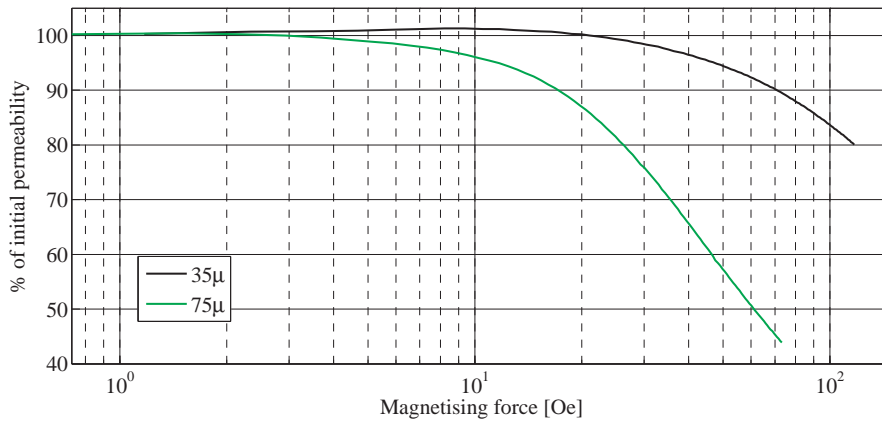


Fig. 5.1 The change in permeability for 35 and 75 $\mu$  iron cores as a function of Oersted.

The ferrite core in figure 5.2 starts to drop at once and has a more smooth drop of compared to the other materials and the reason that the starting value does not start at 100% is because the logarithmic plot does not start at zero. At 50 Oe the permeability has become as low as 10% of the original value which is very low compared to the other materials.

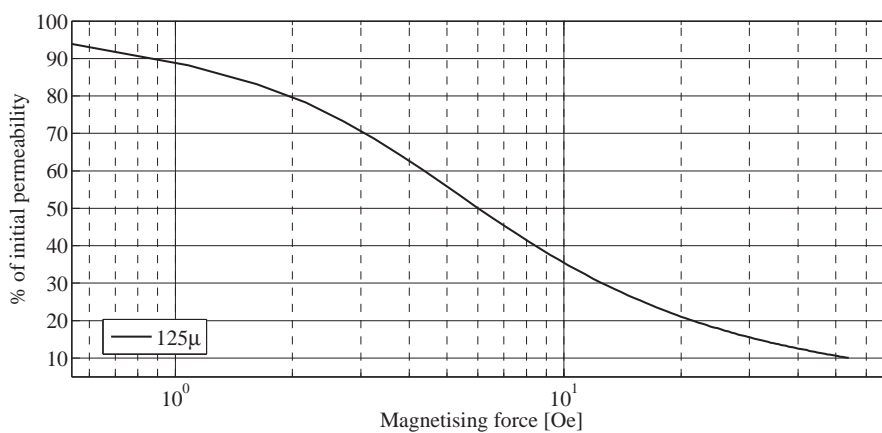


Fig. 5.2 The change in permeability for 125 $\mu$  ferrite core as a function of Oersted.

In figure 5.3 three MPP cores with different permeabilities are shown. It is clear that the lower permeability cores keeps their values longer than the ones with higher initial permeability. They follow the same pattern as the iron cores which is to be expected.

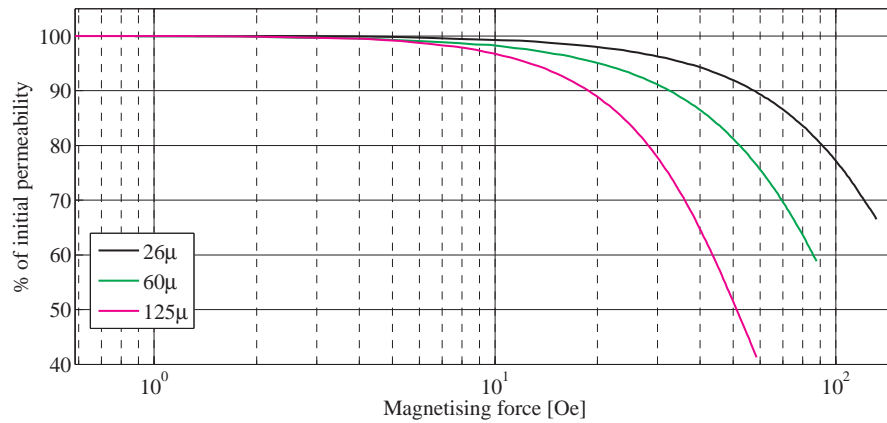


Fig. 5.3 The change in permeability for 26, 60 and 125μ MPP cores as a function of Oersted.

In figure 5.4 three High flux cores with different permeabilities are shown. At 100 Oe the 26μ core still has a permeability above 95% of its initial value and overall the High flux cores can withstand larger magnetising forces than the MPP cores can. This is as expected since the High flux cores are created to be used in high current applications.

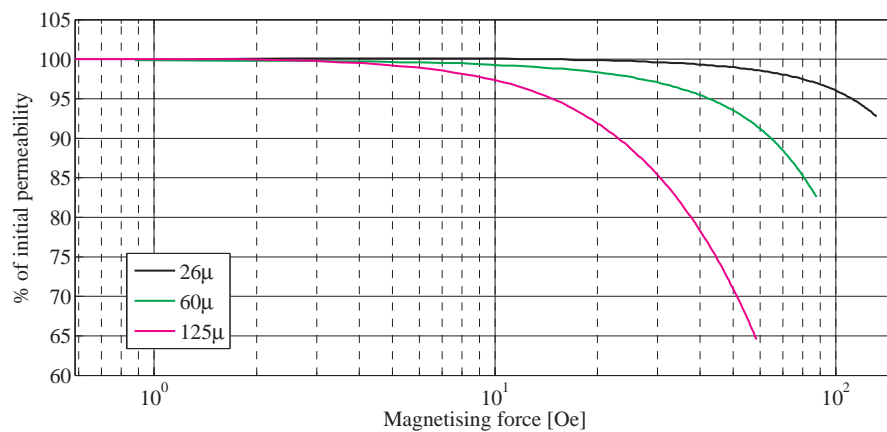


Fig. 5.4 The change in permeability for 26, 60 and 125μ High flux cores as a function of Oersted.

In figure 5.5 two Sendust cores with different permeabilities are shown. Compared to the other powder materials the Sendust cores tends to deviate from their initial values at lower magnetising forces. The shapes are more related to the iron cores and this may be due to the high amount of iron in the powder mix.

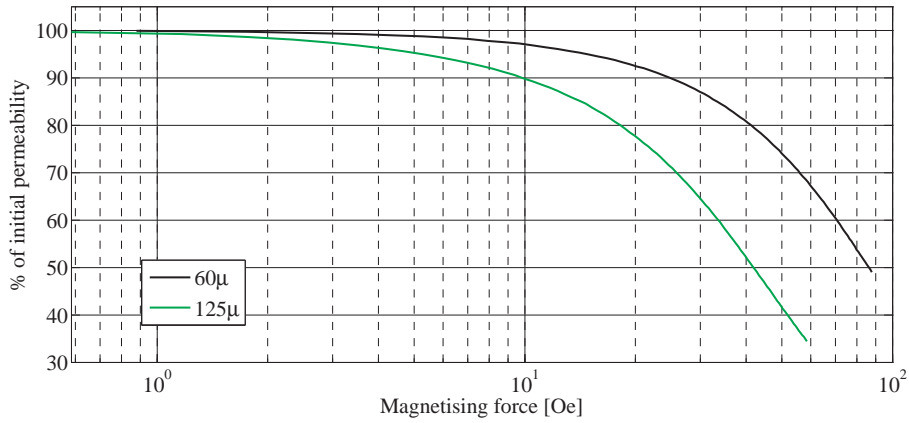


Fig. 5.5 The change in permeability for 60 and 125μ Sendust cores as a function of Oersted.

### 5.2.2 Inductance Changes

For the cores with lower permeabilities and low initial inductance, figure 5.6, the change in inductance is very small with a change of just 10% at 20 A for the MPP cores. This depends on the low amount of turns which yields a low magnetising force. If some turns are added, i.e. by looking at figure 5.7, a much higher drop can be seen, especially for the MPP which drops down to 67% of its initial value. Because of the high magnetic saturation of the High flux, the reduction between 2 μH and 10 μH is low. The peak in the beginning for the iron core is clearly seen for the 10 μH case.

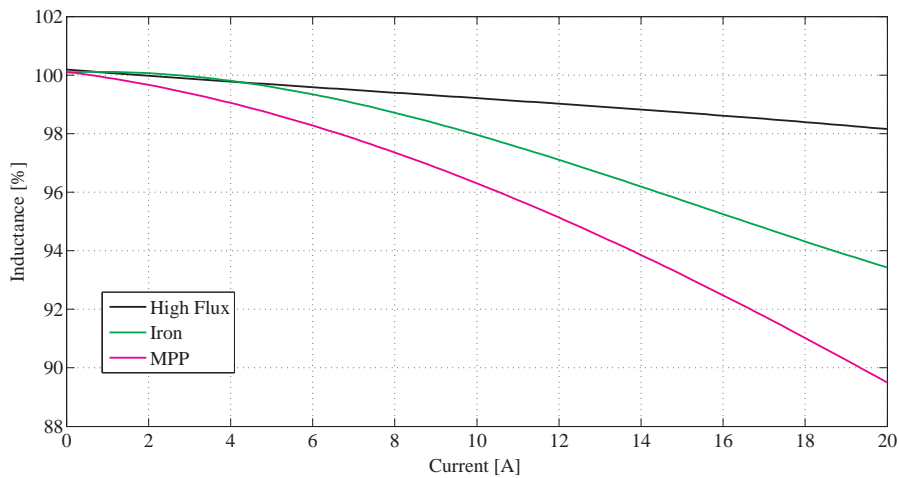


Fig. 5.6 The change in inductance for 26μ MPP and High flux and 35μ cores with a DC-current ranging from 0-20 A. All inductors has an initial inductance around 2μH.

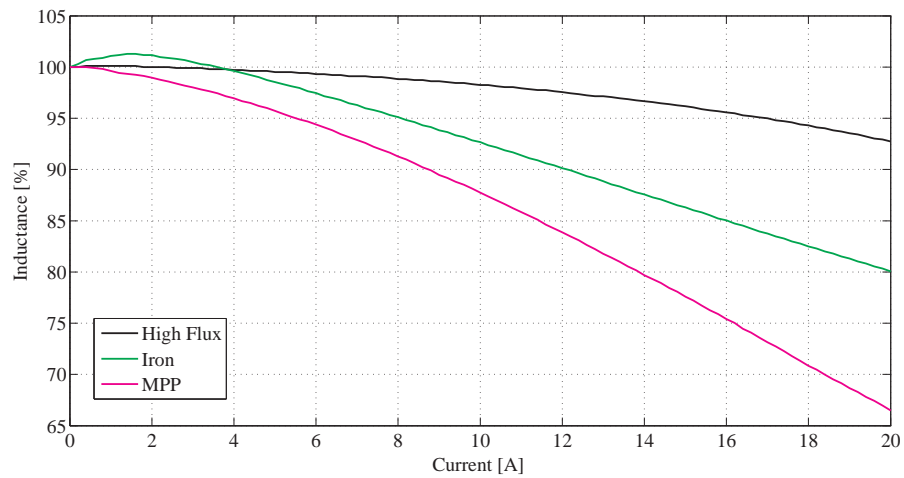


Fig. 5.7 The change in inductance for 26 $\mu$  MPP and High flux and 35 $\mu$  cores with a DC-current ranging from 0-20 A. All inductors has an initial inductance around 10 $\mu$ H.

Figures 5.8 and 5.9 gives a good comparison since all powder materials are present. High flux is yet again the most stable core with the lowest amount of deviations. The iron powder has a higher permeability than the other cores which makes the inductance drop larger than if it had been an 60 $\mu$ , according to figures 5.1-5.5.

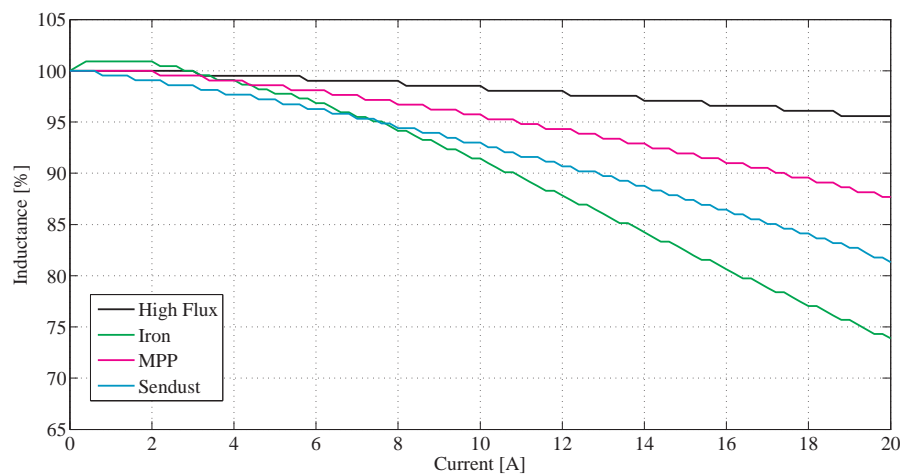


Fig. 5.8 The change in inductance for 60 $\mu$  MPP, Sendust and High flux and 75 $\mu$  cores with a DC-current ranging from 0-20 A. All inductors has an initial inductance around 2 $\mu$ H.

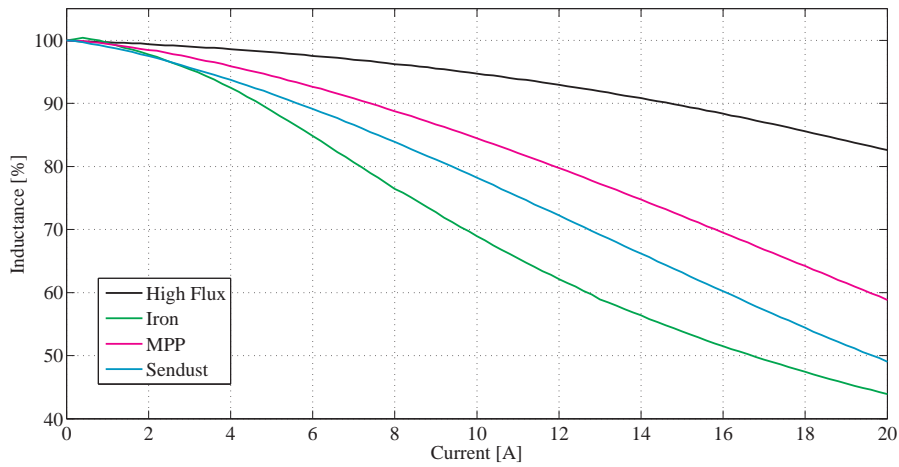


Fig. 5.9 The change in inductance for 60µ MPP, Sendust and High flux and 75µ cores with a DC-current ranging from 0-20 A. All inductors has an initial inductance around 10µH.

In figure 5.10 and 5.11 the 125µ cores are shown and once again the High flux is the best followed by MPP and Sendust. The iron core has a lower permeability than the other materials and it is still not performing better than High flux or the MPP core, except for high currents for the 10 µH case. The reason why iron is added to this plot is because it was the largest permeability available as mentioned in chapter 3 and it will be compared to the other materials in the converter test. The performance of the ferrite is significantly worse than the other core materials.

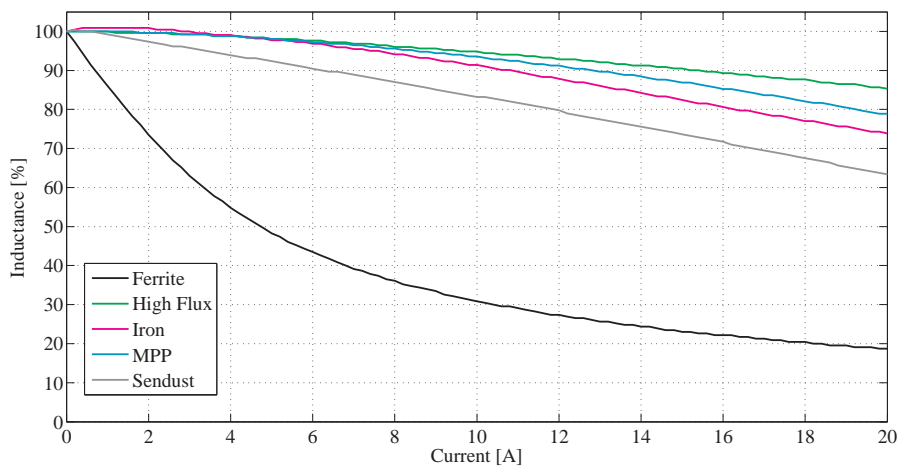


Fig. 5.10 The change in inductance for 75µ iron core and the 125µ MPP, Sendust, High flux and ferrite cores with a DC-current ranging from 0-20 A. All initial inductors has an inductance around 2µH.



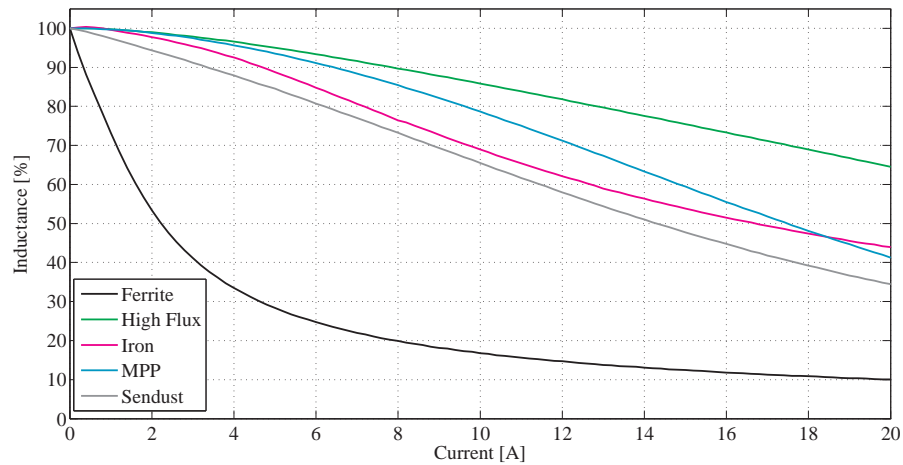


Fig. 5.11 The change in inductance for 75 $\mu$  iron core and the 125 $\mu$  MPP, Sendust, High flux and ferrite cores with a DC-current ranging from 0-20 A. All initial inductors has an inductance around 10 $\mu$ H.

### 5.3 Analysis and discussion

For high magnetising forces, the High flux core is the strongest material since the permeability is kept at a constant high value. The other powder materials has a higher reduction of their permeabilities where MPP is slightly better than Sendust. The iron core is harder to analyse since the permeabilities do not match the other powder cores. The 35 $\mu$  core performs better than the 26 $\mu$  MPP while the 75 $\mu$  iron is not as good as either the 60 and the 125 $\mu$  MPP cores. The ferrite core is in the lower end of the cores as its inductance drops instantaneously and this is due to the ferrites low saturation flux density.

In figures 5.1 - 5.5, all the permeability deviations for the different cores are shown. It can be seen that the higher permeability material changes its permeability both earlier and faster compared to the lower on. This depends on the fact that saturation is reached faster according to (2.7). The ferrite core in figure 5.2 has the highest reduction of its permeability. This was as expected since this type of ferrite core, without air gap, is generally used in low current, high frequency applications.

When looking at figures 5.1 - 5.5 one can think that the lower permeabilities are better than the higher ones since the seem to be more stable. This is not entirely true because it all depends on the application they are used in. As an example by looking at figure 5.3 it can be seen that the effective permeability for the 125 $\mu$  core at 50 Oe is 50% of the initial i.e. 62 $\mu$  compared to the 60 $\mu$  core which has 80% of its initial permeability i.e. 48 $\mu$ . This is important when designing the inductor since a higher permeability material requires less turns and thus less conductor wire. It might also be possible to use a smaller core in that case.

When comparing the measured results with the data sheets acquired from the Magnetics [30] and Micrometals [31] there are some differences. The results can be seen in table 5.1. Generally, the values for the higher permeability are more equal than the lower ones. Magnetics values for their MPP cores tends to be higher than the measured while Micrometals are slightly lower. Both Magnetics and Micrometals seems to underestimate the High flux core and regarding the Sendust the values from Magnetics are a little lower and from Micrometals a bit higher than the measured values. The values from both manufacturer are estimated from their respective graphs and may not be fully accurate.

Chapter 5. DC-Bias Measurements

Table 5.1: Comparison between measured and manufacture values of magnetising force required to reach 90% of initial permeability.

	Measured Value [Oe]	Data Sheet Magnetics [Oe]	Data Sheet Micrometals [Oe]
MPP 26 $\mu$	58	80	44
MPP 60 $\mu$	33	38	32
MPP 125 $\mu$	18.5	17.5	13
High flux 26 $\mu$	100+	100	70
High flux 60 $\mu$	64	50	47
High flux 125 $\mu$	23	23	27
Sendust 60 $\mu$	24	16	30
Sendust 125 $\mu$	10	8	14

## 6. Buck Converter Measurements

In this chapter, the different core materials will be used as an output inductor in a small Buck converter. The frequency as well as the current will be varied and the power will be measured on the input terminal as well as the output terminal.

### 6.1 Test Setup

The efficiency test will be performed with a small buck converter from Texas Instrument, which has a fixed output voltage, 4 V and a maximum output current of 10 A. The input voltage can be varied between 4.5-18 V. The frequency can be set by changing a resistor connected to the drive circuit. The switching frequency was originally put to 300 kHz but by replacing the resistor with a potentiometer the switching frequency can easily be changed. Frequencies between 0.2-1.9 MHz will be used in the tests. A 100 W dynamic load, Chroma 63102, which can handle up to 20 A or 80 V is used in constant voltage mode. The current the load consumes is varied and both the input and output voltages and currents are measured from the buck converter to get the efficiency of the whole circuit. The measurements are performed with a number of Fluke 87 multimeters. The efficiency of the inductor itself is not measured since the board already have existing measurement points for in and output power.

### 6.2 Measurements

All curves presented are mean values of at least three different measurements series. The tests will include permeability comparisons between different materials as well as different permeabilities with the same core material. Output ripple will be measured for the 125 $\mu$  materials as well as both the iron cores and the frequency, a second converter was also used in order to make higher current measurements.

#### 6.2.1 Permeability Comparison

In this section the different materials will be presented one by one and with regards to the various permeabilities. The voltages were put to 12 and 4 V for the input and output voltages respectively. The switching frequency was put to 400 kHz.

Figure 6.1 show the efficiency for the two iron cores and it can easily be seen that the high permeability iron powder has higher losses. This corresponds to the theory mentioned in section 2.3 which states that the core losses should be larger for the higher permeability material.

Chapter 6. Buck Converter Measurements

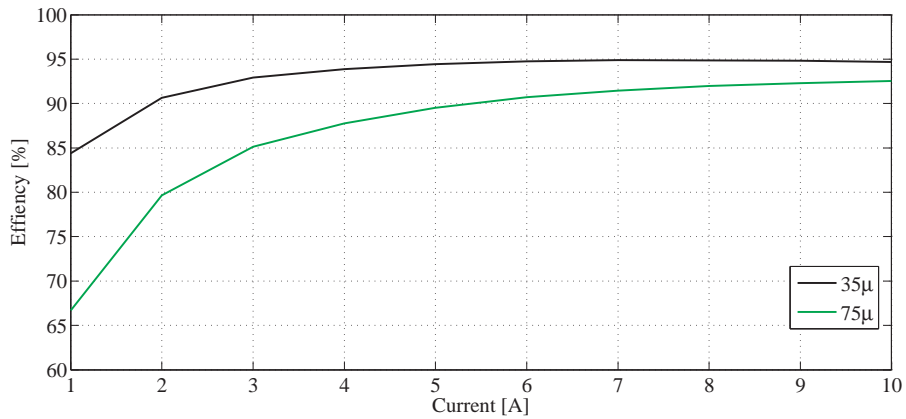


Fig. 6.1 The efficiency of the buck converter as a function of output current for two iron cores with different initial permeabilities.

Figure 6.2 shows that the core losses for the three MPP cores. Overall it can be seen that the different permeabilities keep up with each other due the low core losses in the MPP material and thus the difference between them are low.

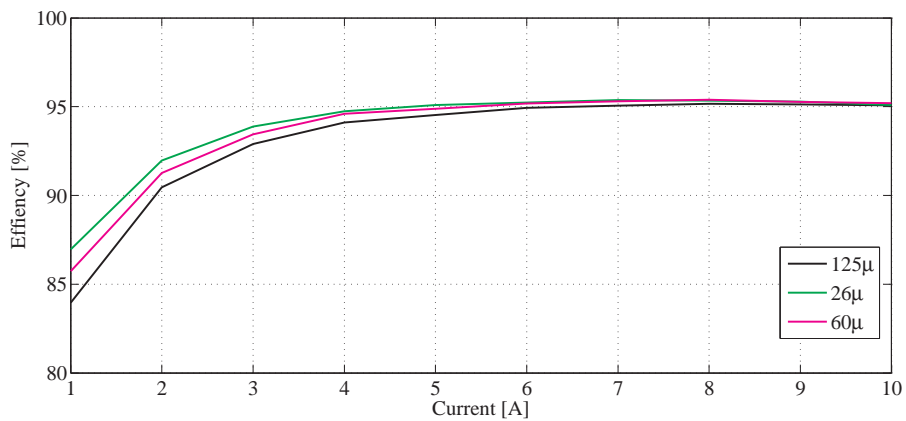


Fig. 6.2 The efficiency of the buck converter as a function of output current for three MPP cores with different initial permeabilities.

The difference between the High flux cores, seen in figure 6.3, is more apparent than the MPP cores. The efficiency of the High flux cores has a higher spread than the MPP cores for lower currents. The shape of the 26μ core is different than the other curves in the fact that it starts to decline at 6 A.

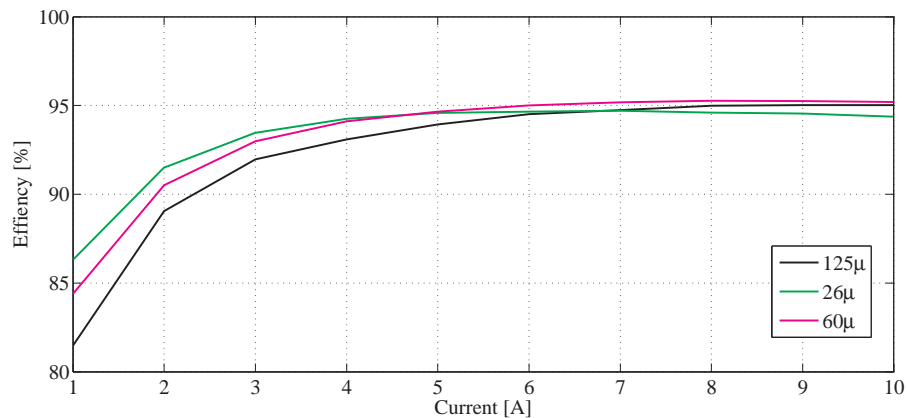


Fig. 6.3 The efficiency of the buck converter as a function of output current for three High flux cores with different initial permeabilities.

In figure 6.4 the performance of the Sendust cores are shown and they follow the same pattern as for the other materials i.e. the lower permeability material perform better and the curve shapes behave similarly.

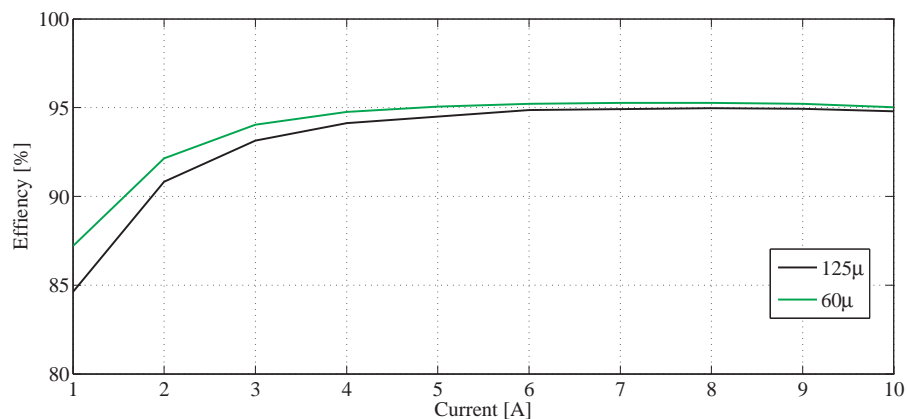


Fig. 6.4 The efficiency of the buck converter as a function of output current for two Sendust cores with different initial permeabilities.

## 6.2.2 Material Comparison

This section will compare the different materials with the same permeabilities against each other. The 75μ iron will be compared against the 125μ as well as the 60μ. The comparisons will be performed with the same buck converter as in 6.2.1. The input voltage was put to 12 V and the output voltage was fixed at 4 V. The frequency was put to 400 kHz. The voltage ripple on the output of the buck converter will be measured for the 125μ material, since these has the largest ripple due to the higher inductance reduction. The 125μ materials has also been tested with a sweep of the switching frequency between 0.2-1.9 MHz.

Figure 6.5 shows all the 60μ material and both of the iron powders. It can clearly be seen that the 75μ has a much lower efficiency than all the other materials and this is due to higher core losses. When looking at the other materials one will notice that Sendust is the most efficient material at lower currents followed by MPP and High flux. When the current increases all the material move towards each other except for the iron which is slightly lower than the other powder materials.

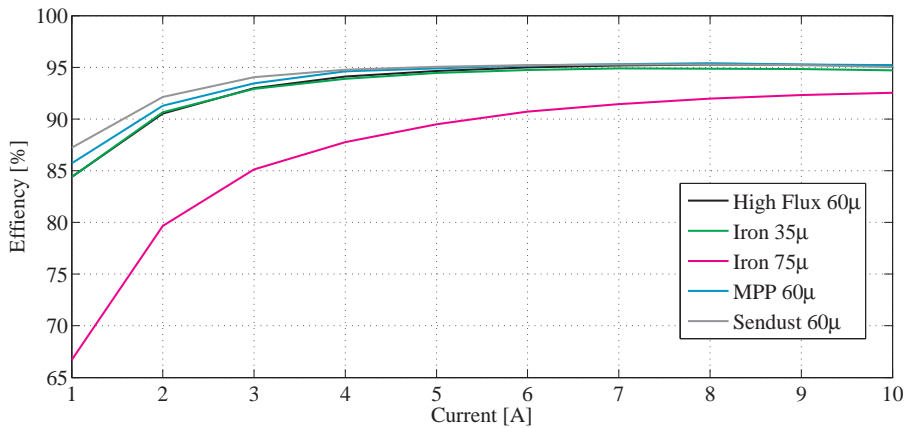


Fig. 6.5 The efficiency of the buck converter as a function of output current for all 60µ material as well as the 75µ and 35µ iron.

In figure 6.6 the different 125µ materials are presented as well as the 75µ iron. Even though the iron core has a lower permeability its performance is still significantly lower than the rest of the materials. Sendust has the highest efficiency across the whole current spectrum and the performance of the rest of the materials have similar performance.

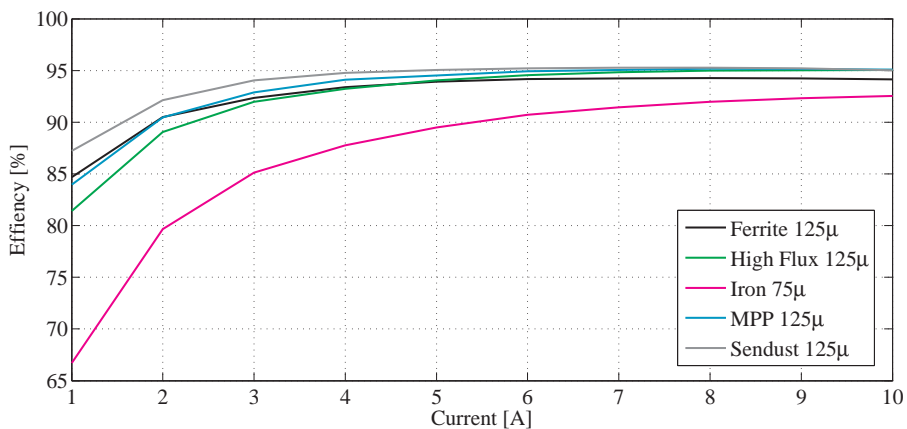


Fig. 6.6 The efficiency of the buck converter as a function of output current for all 125µ material as well as the 75µ iron.

### Ripple Measurement

The ripple measurement was made with an input voltage of 12 V, an output current of 10 A and switching frequency 400 kHz. The ripple in the voltage occurs because of the ripple current according to (2.1) and the results for the 75µ iron and all the 125µ cores can be seen in figure 6.7.

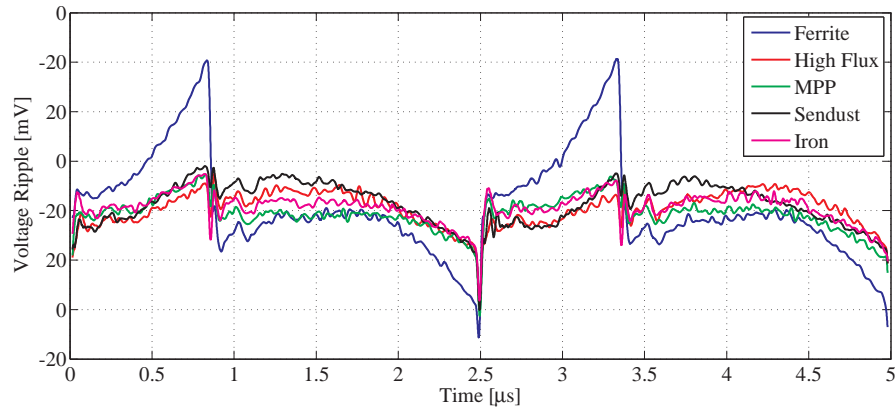


Fig. 6.7 The output voltage ripple for all 125 $\mu$  materials as well as the 75 $\mu$  iron.

At time zero the switch is turned on and the voltage level increases until the switch is turned off at the peak at 0.8  $\mu$ s. The ripple for the materials has equal looking waveforms, when it comes to the shape. Sendust has a slightly higher ripple than the other powder material and this can be explained by the fact that its inductance drops a bit more. The reason that the ripple in the ferrite core is as high as it is depends on the fact that this core is close to its saturation meaning that the initial inductance of 2  $\mu$ H has been greatly reduced. The small swing that will occur in the flux density will give rise to a high change in the ripple current. There are two possibilities to decrease the output ripple. First, one can increase the inductance of the inductor, this will give higher resistive losses since more copper wire is needed, or a higher output capacitance can be used.

### 6.2.3 High Current Buck Converter

In this section a different buck converter which can provide 25 A output will be used to evaluate the materials. In this case the inductor will be slightly over dimensioned due their size which makes it difficult to lower the inductance. The switching frequency for the tests is 500 kHz, the input voltage 14 V and the output voltage 1 V. Figure figure 6.8 shows the performance of the MPP cores and figure 6.9 shows the High flux cores.

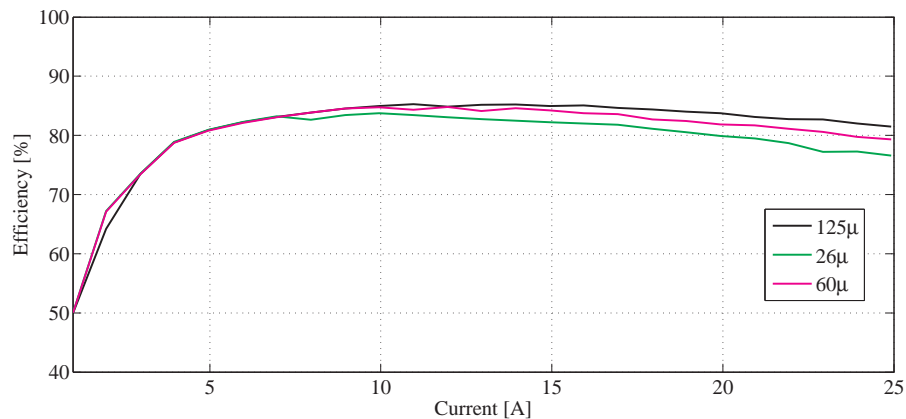


Fig. 6.8 The efficiency of the buck converter as a function of output current for three MPP cores with different initial permeabilities when the current is increased to 25 A.

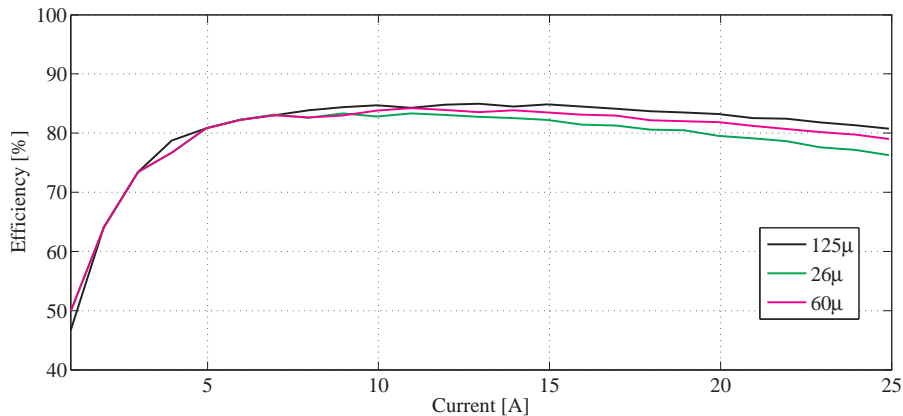


Fig. 6.9 The efficiency of the buck converter as a function of output current for three High flux cores with different initial permeabilities when the current is increased to 25 A.

One can clearly see that in this case the core losses are significantly lower due to the rather high inductance value which can be seen because all the cores have similar efficiency at the lower currents when compared to figure 6.2. This becomes very clear at 7 A where the resistive losses takes over for the 26μ which starts to lose efficiency compared to the other two cores. The 60μ follow the same pattern at 7 A. Here it is clear that the trade of between high inductance and resistive losses should be considered when designing a DC-choke.

### 6.2.4 Frequency Sweep in Buck Converter

In this test the frequency has been swept from 0.2-1.9 MHz with an input voltage of 18 V, an output voltage of 4 V and a current of 10 A. The test was performed with all 125μ cores and 75μ iron core since all the different materials where present. It is important to note that the differences between the material is not only dependent on the frequency since they behave different for high current. Another factor with an increasing frequency is that the inductor itself becomes over dimensioned since the ripple decreases. This will have the effect that the material characteristics becomes more equal since the AC flux shrinks and the results can be seen in figure 6.10.

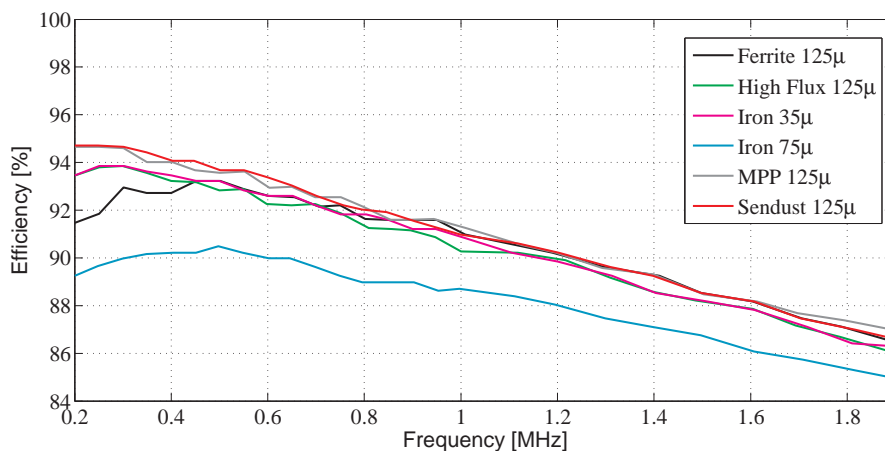


Fig. 6.10 The efficiency for all 125μ material as well as the 35μ and 75μ iron when the switching frequency is swept in the Buck converter.

One of the first things to notice is that the difference between the different materials is largest for lower



frequencies. Sendust and MPP has the best performance but except from the 75 $\mu$  iron all materials has similar curves. All materials has its efficiency declining with higher frequencies and this is because of the increased switching losses in the converter and not specifically in the inductor.

### 6.3 Analysis and discussion

All materials except 75 $\mu$  iron have similar results but Sendust and MPP have a slightly better performance than the other materials. The largest differences can be seen for lower frequencies and low currents. The reason for the similar performance is that the majority of the losses is located in the copper wires and the other parts of the converter. This is easiest seen in figures 6.8 and 6.9 where most of the difference above 7 A is because of the larger copper resistance for the lower permeability materials.

When focusing on the lower currents it is seen that the High flux core has lower efficiency which corresponds to the higher core losses. The performance for the High flux increases with an increase of the output current in regards to both MPP and Sendust. This mainly depends on the fact that the High flux core keep its inductance value, i.e. the core losses of MPP and Sendust increases. The performance of MPP and Sendust is similar for all currents tested. This depends on that both material has low core losses but mostly that the buck converter give rise to a low flux swing. For currents above 6 A, the High flux core perform as well as the MPP and Sendust cores.

The ferrite core performs as the other materials for lower currents, mostly because of its very low core losses, but as the current increases the inductance will drop quickly, see figure 5.10. Even though the ferrite core has a good efficiency, a drawback is that the ripple across the load is a lot higher than the other materials which can be seen in figure 6.7.



## 7. BH-curve Measurements

The content of this chapter includes measurements of the BH-curve for the different materials. Core losses for 10 kHz has also been measured.

### 7.1 Test Setup

The BH-curve of the core materials will be measured by putting two separate windings on the inductor core. The primary core will create the magnetising force and the secondary winding will be used for measuring the voltage. The inductor will be fed by an AC voltage from a custom made amplifier available at the site. The current will be measured with a current probe, Lecroy A015, at the primary side and the voltage curve will be measured by an oscilloscope at the secondary side. The full setup can be seen in figure 7.1.

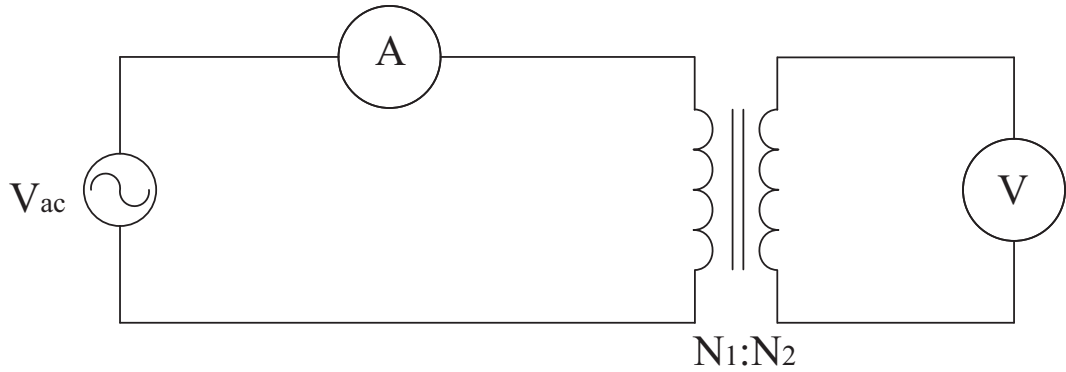


Fig. 7.1 Schematics for the setup of the BH-curve measurements.

The cores has been wound uniformly across the surface of both the primary and secondary side, this to make the fields more uniform. This will also improve the coupling between the two windings. The magnetising force can be calculated from equation (2.10) as

$$H = \frac{N_1 i}{l} \quad (7.1)$$

where  $N_1$  is the number of turns on the primary winding,  $i$  is the current in the winding and  $l$  is the mean magnetic path of the inductor core. The flux density will be calculated from the output of the secondary winding as

$$B = \frac{1}{AN_2} \int V_L dt \quad (7.2)$$

where  $A$  is the cross sectional area of the core,  $N_2$  is the number of turns on the secondary winding and  $V_L$  is the voltage of the secondary winding [32]. To reach the saturation levels a high amount of turns are needed on the primary winding as well as a high current.

The reason for measuring at the secondary side is to reduce the effect of the resistive voltage drop on the primary side. No current flow at the secondary side, because of the  $1 \text{ M}\Omega$  impedance of the Oscilloscope, which implies that the voltage on the secondary side only is affected by the magnetising current [33].

For practical reasons the 26 $\mu$  and the 35 $\mu$  will not be measured because of the high number of turns that is necessary to reach saturation. For the other cores refer to Table 7.1 for primary and secondary windings. Note that the primary winding may differ a bit from the initial value due to the human factor when manually winding the cores.

Table 7.1: Turns

	Primary	Secondary
60 $\mu$	130	30
75 $\mu$	100	22
125 $\mu$	75	15

When the core losses were measured the same amount of turns was wound on both the primary and the secondary coil of the core because then no transformation between the two sides are necessary. The number was chosen to 30 turns each and the core loss is calculated as

$$P = \frac{V_{secondary} I_{primary}}{Volume} \quad (7.3)$$

where  $V_{secondary}$  is the voltage of the secondary side,  $I_{primary}$  is the current on the primary side and  $Volume$  is the volume of the core.

## 7.2 Results

In this section the BH-curve measurements will be evaluated. The material will be compared permeability against permeability.

### 7.2.1 BH-curve

Figure 7.2 shows the BH-curves for the 60 $\mu$  cores as well as the 75 $\mu$  iron. In the linear region it can be seen that the materials show the same slope which is predicted since the permeability should keep its value in that region.

When comparing MPP and Sendust, one can see that they have very similar shapes although the Sendust slope starts to flatten earlier than the MPP. When looking at the higher magnetising force one can see that the Sendust core rises above the MPP. Since the Sendust core starts to flatten earlier it means that its permeability starts to decline earlier than the MPP and this can also be seen in figure 5.9. Since the Sendust gets a slightly higher flux density at higher magnetising forces, this would imply that the saturation flux would be higher, but this could not be tested due to limitation of the equipment.

When looking at the High flux core it is clear that the saturation flux is much higher than for MPP and Sendust. This was no surprise since the High flux core has its name because of its high flux density. The iron has not the same shape in the linear region as the other material since it has a different initial permeability. One can see that the iron starts to flatten around the same value as the Sendust but at a faster pace. On the other hand the flux density is much higher than any of the other materials.

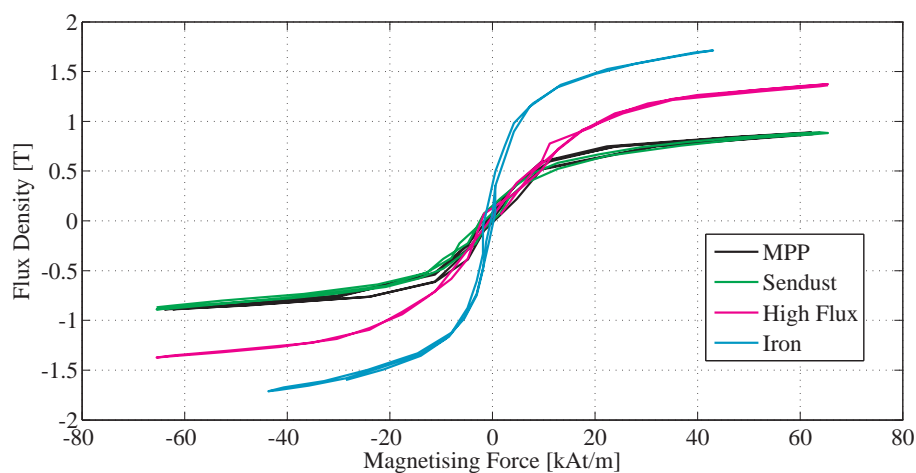


Fig. 7.2 The BH-curves for 60 $\mu$  MPP, Sendust and High flux cores and 75 $\mu$  iron core.

When looking at the 125 $\mu$  materials in figure 7.3 a different pattern can be seen for the Sendust and MPP core. In this case one clearly sees that the Sendust starts to flatten way before the MPP and that the shapes do not look as similar as for 60 $\mu$  cores. When the magnetising force gets higher it can be seen that the Sendust core starts to get closer to the MPP core. For the 125 $\mu$  Sendust it may reach its saturation at 1 T since it keeps on rising even at the high magnetising force. Once again the High flux core has a higher flux density and by looking at the shape of the curve it seems that the saturation flux can be as high as 1.5 T. When looking at the ferrite one can see that curve starts to flatten very fast and that the saturation flux density is around 0.5 T, this is higher than for many other ferrites which often is said to have saturation at around 0.3 T. The different slope of the 125 $\mu$  ferrite core depends on a slightly different geometry than the 125 $\mu$  materials.

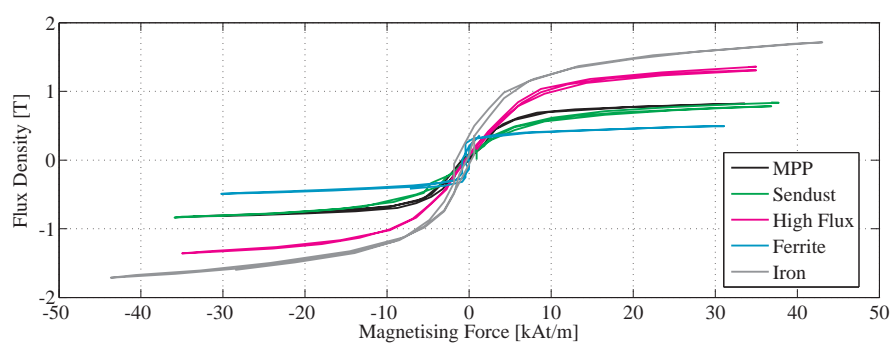


Fig. 7.3 The BH-curves for the 75 $\mu$  iron core and 125 $\mu$  MPP, Sendust, High flux and Ferrite cores.

## 7.2.2 Core losses

The core losses was measured at a frequency of 10 kHz. Attempts at higher frequencies were made but the voltage required to get the amount of current needed could not be obtained with amplifier used. The ferrite core has been excluded from this test due to its low saturation.

In figure 7.4 the core losses for the 125 $\mu$  cores and the 75 $\mu$  iron core are presented. The MPP and Sendust cores are located close to each other with High flux and iron followed above.

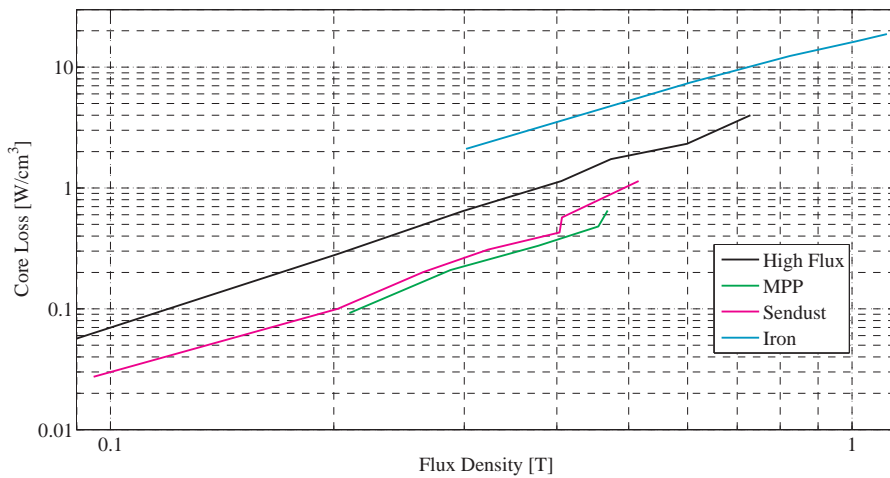


Fig. 7.4 The measured core losses as a function of the flux density for the 75 $\mu$  iron core and 125 $\mu$  MPP, Sendust and High flux cores at 10 kHz.

In figure 7.5 the core losses for the 60 $\mu$  cores and the 35 $\mu$  iron core are presented. The curves follow the same pattern as for the 125 $\mu$  with the small exception that the High flux core is closer to both Sendust and MPP.

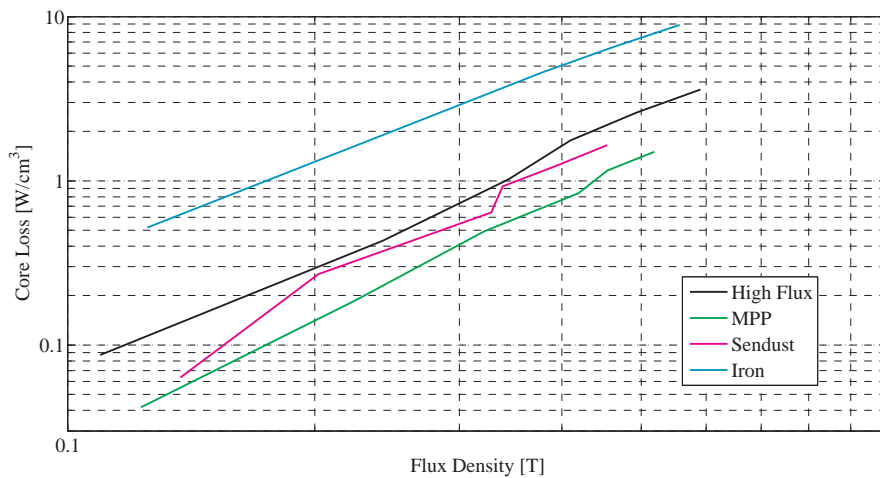


Fig. 7.5 The measured core losses as a function of the flux density for the 60 $\mu$  cores and the 35 $\mu$  at 10 kHz.

### 7.3 Analysis and Discussion

Overall one can see that all materials have thin BH-curves which is the case for soft magnetic materials as mentioned in section 2.3. One interesting observation is that the MPP and Sendust cores have similar shapes as well as limits to their respective flux density at around 0.8 T which is where the MPP core should have its limit. However, the Sendust core should saturate at 1 T according to the manufacturers and this is conclusive for both the 60 $\mu$  and the 125 $\mu$  permeabilities. The High flux core is also a bit lower than its expected value at 1.5 T but as seen in figures 7.2 and 7.3 the slope has not yet flattened which still makes it possible for it to reach its expected value.

When it comes to core losses the materials are located in the expected order which is MPP, Sendust, High flux and iron where the lowest core losses are mentioned first. The core losses matches the manufactures data sheet [34] well for the frequency used. One interesting result is that the losses are higher for the low permeability materials and the same phenomenon can be seen when studying the data sheets for the cores at this low frequency. This pattern changes at higher frequencies and thus the higher permeability cores will have higher losses. In table 7.2 the losses at 0.3 T are presented. Note that the manufacture did not have any values for Sendust at 10 kHz available.

Table 7.2: Core loss comparison between measured and manufacture values at 0.3 T.

	Measured Value [ $\text{W}/\text{cm}^3$ ]	Data Sheet Magnetics [ $\text{W}/\text{cm}^3$ ]
MPP 60 $\mu$	0.4	0.5
MPP 125 $\mu$	0.23	0.175
High flux 60 $\mu$	0.7	0.7
High flux 125 $\mu$	0.65	0.42
Sendust 60 $\mu$	0.55	-
Sendust 125 $\mu$	0.27	-

If one compares the core losses figures with the BH-curve figures one can see that the MPP and Sendust graphs are close to each other in all figures. As explained in section 2.1.1 the losses is the movement in the BH-curve and this seems to correspond well between the two measurements.





## 8. Categorisation

When analysing the measurements some trends are very clear and comprehensive across all tests. The first one is that High flux has an excellent DC-bias performance where the inductance keeps a high value even when stressed with high magnetising forces. A drawback with the High flux is that it has lower efficiency in the buck converter test for lower currents, compared to Sendust and MPP, because of its higher core losses.

When looking at the two powder materials with the lower core losses, MPP and Sendust, one can clearly see that they are in league with the standard ferrite. One interesting thing is that Sendust cores performed better than MPP for all buck tests with high ripple, which was a bit surprising since the manufactures always promotes MPP as a lower core loss material, see 7.2.2. The 75 $\mu$  iron core had the overall worst performance of all the cores. It was especially obvious in the buck tests where it was not even close to the other materials. The reason for this is not clear and parallels can not be drawn to other types of iron cores.

All the tested materials followed the same trend when it comes to core losses for different permeabilities, higher permeability yields higher core losses, but the resistive losses will at some point be the major loss factor. When it comes to storage vs size it is important that the inductor can handle High flux density according to (2.8) since the flux density is dependent on the effective area of the core. So if the designer want to reduce the size of the core but still maintain the inductance one must choose a core material with high saturation flux density or a material that keeps the inductance even if the current goes up.

By looking at the material in this thesis, to keep a high inductance one might use the iron which has a really high saturation flux which will keep the inductance even for small cores. An even better alternative would be the High flux core, although it has a lower saturation flux density but the permeability will be higher due to that its BH-curve starts to flatten for higher magnetising forces than the iron. Another way is to use a higher permeability which will yield in higher inductance per turn of wire according to (2.14). This will cause one problem if the current gets to high since higher permeability will decrease faster than the lower one. If one would want higher permeability MPP would be a good choice since it has a permeability range up 550 $\mu$ .

For high current applications with low frequencies below 50 kHz iron would be preferred due to its high saturation flux density and low cost since the low frequency will keep the losses down. If the frequency goes up then High flux would be preferred because of the high current. For frequency higher than 500 kHz one would have to choose between MPP and Sendust and if the current is too high MPP will not be a good solution since it has lower saturation flux density than Sendust according to the manufactures, although it has not been confirmed in this thesis. If the frequency reaches a couple of MHz, ferrites would be the only choice but then an air gap has to be introduced, alternatively one could increase the area of the core but that will make the inductor larger which could be a limiting factor.

For buck converters it is, as mentioned, important to have an inductor which can handle high current and is not so dependent of the switching frequency. The test in chapter 6.1 shows that most material can keep the efficiency high but with different output ripple due to reduced inductance. The material that overall were the best was Sendust and this core was also one of the cheapest which would make it a good choice for a DC-choke. This is because of its rather high saturation flux and low core losses.

When it comes to low current applications most of the materials can be used, and in this case it may be

## *Chapter 8. Categorisation*

a good idea to use lower permeability because the resistive losses will be lower and instead core losses will be more dominant. Lower permeability has been shown in the thesis to give higher core losses at low frequencies. In this case it can be suitable to use a iron powder core up to some kHz since the losses are lower. Otherwise, if the frequency goes up it is suitable to ferrite since if the current is low, the ferrite will not reach saturation. If the inductance has to be larger MPP and Sendust would be good choice.

Overall one can say that all the powder material has good performance when it comes to high currents, especially when compared to ferrites. One drawback for the powder materials is their limited core shapes where both MPP and High flux are limited to toroidal, while iron powder and Sendust comes in more shapes which can be good for a designer with special needs for a design.

Another issue for powder materials is the cost of the cores. A lot of the cores has high nickel content as well as a costly manufacturing process. When talking to various suppliers of standard inductors, which was performed when trying to get hold of test samples, most of them expect that they will not start to make standard components from MPP and High flux in the near future. Most of them promotes their iron powder since it is easier to work with, the cost for material is much cheaper and the demand is higher. The manufacturers say that they are not willing to invest in the machinery necessary to make MPP and High flux due to its cost and limited market for those materials.

Due to aging of the iron powder binders it would not be recommended to use this material for long term applications, where instead ferrite and the other powder materials does not age in the same way. When designing an application which should last for many years then it would preferred to avoid the iron powder because of its organic binder.

## **9. Conclusion**

The powder materials tested shows good performance in all tests that has been conducted in this thesis. The results confirm that the alternative materials fits in the frequency region between where iron and ferrite cores has their best performance. The powder materials are suitable as output inductors in DC-DC applications which can be seen in chapter6. The High flux cores had the best performance with high DC-current whereas Sendust had the best performance with higher frequencies. The MPP material had the lowest core losses. According to the BH-curve tests, Sendust and to some point High flux did not reach their specified flux density limits. Sendust have been the material that has had the best overall performance. Other positive aspects with Sendust is that it is the cheapest of the new powder material and the core can be made in other shapes than toroidal.

### **9.1 Future Work**

In order to be able to use the powder material in commercial applications the temperature limits of the materials has to be investigated, especially the long term stresses under high temperature has to be studied. There would also be a need to optimise the inductor design in a specific application and compare these with the materials used today, for instance with gapped ferrite cores since they have not been compared in this thesis. Another aspect to consider is the possibility of creating adequate spice models for the different material which can be a helpful asset in the design process.



## References

- [1] M. W. Horgan, "Inductor core technology: Shrinking power supplies," *Power Electronics Technology*, vol. 28, July 2002.
- [2] G. L. Johnson, *Solid State Tesla Coil*, October 2001.
- [3] D. K. Cheng, *Field and Wave Electromagnetics*, 2nd ed. Addison-Wesley, 1989.
- [4] A. I. Pressman, *Switching Power Supply Design*, 3rd ed. McGraw-Hill, 2009.
- [5] W. T. McLyman, *Transformer and Inductor Design Handbook*, 4th ed. Taylor and Francis Group, LLC, 2011.
- [6] H. Johnson. Skin effect calculation. Accessed 2013-04-11. [Online]. Available: <http://www.sigcon.com/Pubs/misc/skineffect-calculations.htm>
- [7] N. Mohan, T. M. Undeland, and W. P. Robbins, *Power Electronics: Converters, Applications and Design*, 3rd ed. John Wiley and Sons, 2002.
- [8] "Magnetics all products bulletin," Magnetic Inc., 2011, product Bulletin.
- [9] N. J. Schade, "Core losses in composite inductors," Design Handbook, Vishay Intertechnology, Inc. [Online]. Available: <http://ecadigitalibrary.com/pdf/CARTSEUROPE06/3.6%20Shade.a.pdf>
- [10] "Soft ferrites and accesories," Ferroxcube, 2008.
- [11] Learn more about ferrite cores. Magnetics, Inc. Accessed 2013-04-12. [Online]. Available: <http://www.mag-inc.com/products/ferrite-cores/learn-more-about-ferrites>
- [12] Learn more about powder cores. Magnetics, Inc. Accessed 2013-07-04. [Online]. Available: <http://www.mag-inc.com/products/powder-cores/learn-more-about-powder-cores>
- [13] "Using magnetic cores at high temperature, cg-06," Magnetics, Inc, technical Bulletin.
- [14] "Powder cores catalog," Magnetics, Inc, 2012, product Catalog.
- [15] Iron powder cores. KDM Co.Ltd. Accesed 2013-07-04. [Online]. Available: <http://www.kdm-mag.com/products/Iron-Powder-Cores1/>
- [16] "Section i: Iron powder cores," Amidon,Inc, accessed 2013-07-04. [Online]. Available: [http://www.amidoncorp.com/product\\_images/specifications/1-02.pdf](http://www.amidoncorp.com/product_images/specifications/1-02.pdf)
- [17] Whats new. Micrometals. Accesed 2013-07-04. [Online]. Available: [http://www.micrometals.com/whatsnew\\_index.html](http://www.micrometals.com/whatsnew_index.html)
- [18] T.Slatter, "A comparson of molybdenum permalloy powder and sendust cores for energy storage inductors." Arnold Engineering company, May 2000.
- [19] "Micrometals arnold powder cores catalog," Micrometals Arnold Powder cores, 2012, product Catalog.

## References

- [20] "Learn more about high flux cores," Magnetics Inc., accessed 2013-05-31. [Online]. Available: <http://www.mag-inc.com/products/powder-cores/high-flux-cores/learn-more-high-flux>
- [21] "Magnetics powder cores," Magnetics Inc., accessed 2013-05-31. [Online]. Available: <http://www.mag-inc.com/products/powder-cores>
- [22] M. A. Willard and M. Daniil, "Nanostructured soft magnetic materials," in *Nanoscale Magnetic Materials and Applications*, J. P. Liu, E. Fullerton, O. Gutfleisch, and D. J. Sellmyer, Eds. Springer US, 2009.
- [23] M. Ferch, "Softmagnetic materials in todays power electronic designs," Magnetec, 2000, technical Bulletin.
- [24] Htc iron powder core. Manz Electronic Systeme OHG. Accessed 2013-04-15. [Online]. Available: [http://www.manz-electronic.com/product\\_htc-iron-powder-cores\\_20.html](http://www.manz-electronic.com/product_htc-iron-powder-cores_20.html)
- [25] Thermal aging. Micrometals, Inc. Accessed 2013-07-04. [Online]. Available: [http://www.micrometals.com/thermalaging\\_index.html](http://www.micrometals.com/thermalaging_index.html)
- [26] Taf200. Curie Industrial. Accessed 2013-04-15. [Online]. Available: <http://www.curie.com.tw/p2-material-1.asp>
- [27] J. Smith, "Self-resonant frequency of an inductor," Clifton Laboratories, accessed 2013-08-20. [Online]. Available: [http://www.cliftonlaboratories.com/self-resonant\\_frequency\\_of\\_inductors.htm](http://www.cliftonlaboratories.com/self-resonant_frequency_of_inductors.htm)
- [28] "Permeability vs frequency curves for powder cores," Magnetic Inc., accessed 2013-08-20. [Online]. Available: <http://www.mag-inc.com/products/powder-cores/permeability-versus-frequency-curves-for-powder-cores>
- [29] "Permeability v. frequency curves for mpp, hi-flux, smss cores," Micrometals, 2011, product Bulletin.
- [30] "Permeability vs dc-bias curves for powder cores," Magnetic Inc., accessed 2013-08-20. [Online]. Available: <http://www.mag-inc.com/products/powder-cores/permeability-versus-dc-bias-curves-for-powder-cores>
- [31] "Permeability v. dc bias curves for mpp, hi-flux, smss cores," Micrometals, 2011, product Bulletin.
- [32] W. Soong, "Bh-curve and iron loss measurement for magnetic materials," Power Engineering Briefing note series, School of Electrical and Electronic Engineering, University of Adelaide, 2008.
- [33] Y. Han, W. Eberle, and Y.-F. Liu, "New measurement methods to characterize transformer core loss and copper loss in high frequency switching mode power supplies." in *35th Annual IEEE Power Specialists Conference*. Queen's University at Kingston, 2004.
- [34] "Core loss density curves for powder cores," Magnetic Inc., accessed 2013-08-20. [Online]. Available: <http://www.mag-inc.com/products/powder-cores/core-loss-density-curves-for-powder-cores>